Journal of Theoretical Biology 376 (2015) 118–133

Contents lists available at ScienceDirect

Journal of Theoretical Biology

journal homepage: www.elsevier.com/locate/yjtbi

The role of skeletal muscle in liver glutathione metabolism during acetaminophen overdose

L.M. Bilinsky [a,*], M.C. Reed [a], H.F. Nijhout [b]

[a] Department of Mathematics, Duke University, United States
[b] Department of Biology, Duke University, United States

HIGHLIGHTS

- We have devised a mathematical model of glutathione (GSH) metabolism in liver.
- We include glutamine (Gln, a GSH precursor) synthesis/export by skeletal muscle.
- We explain the linear decline in muscle Gln accompanying elevated plasma cortisol.
- Sterile inflammation and system x_c^- in liver aid GSH recovery after APAP overdose.
- Giving glutamine (in addition to NAC) may be beneficial during APAP overdose.

ARTICLE INFO

Article history:
Received 30 October 2014
Received in revised form
29 March 2015
Accepted 6 April 2015
Available online 16 April 2015

Keywords:
Mathematical model
Catabolic state
Dexamethasone
Cystine–glutamate antiporter
Sterile inflammation
Glutamine supplementation

ABSTRACT

Marked alterations in systemic glutamate–glutamine metabolism characterize the catabolic state, in which there is an increased breakdown and decreased synthesis of skeletal muscle protein. Among these alterations are a greatly increased net release of glutamine (Gln) from skeletal muscle into blood plasma and a dramatic depletion of intramuscular Gln. Understanding the catabolic state is important because a number of pathological conditions with very different etiologies are characterized by its presence; these include major surgery, sepsis, trauma, and some cancers. Acetaminophen (APAP) overdose is also accompanied by dramatic changes in systemic glutamate–glutamine metabolism including large drops in liver glutathione (for which glutamate is a precursor) and plasma Gln. We have constructed a mathematical model of glutamate and glutamine metabolism in rat which includes liver, blood plasma and skeletal muscle. We show that for the normal rat, the model solutions fit experimental data including the diurnal variation in liver glutathione (GSH). We show that for the rat chronically dosed with dexamethasone (an artificial glucocorticoid which induces a catabolic state) the model can be used to explain empirically observed facts such as the linear decline in intramuscular Gln and the drop in plasma glutamine. We show that for the Wistar rat undergoing APAP overdose the model reproduces the experimentally observed rebound of liver GSH to normal levels by the 24-h mark. We show that this rebound is achieved in part by the action of the cystine–glutamate antiporter, an amino acid transporter not normally expressed in liver but induced under conditions of oxidative stress. Finally, we explain why supplementation with Gln, a Glu precursor, assists in the preservation of liver GSH during APAP overdose despite the fact that under normal conditions only Cys is rate-limiting for GSH formation.

1. Introduction

The liver is the major site of amino acid metabolism, and the organ in which most glutathione (GSH) synthesis occurs; GSH is often referred to as the "master antioxidant," and has a major role in protection against oxidative stress and removal of xenobiotics. Glutamate (Glu) is one of the three amino acid precursors of GSH and also occupies a central role in the breakdown of dietary amino acids entering the liver via the portal vein by serving as an intermediate in the disposal of amino groups via urea. In the course of this process, Glu is interconverted with α-ketoglutarate, an intermediate in the tricarboxylic acid (TCA) cycle. The liver does not take up Glu directly but obtains it by uptake and deamination of glutamine (Gln). Skeletal muscle is the primary site of Gln synthesis and a major exporter of Gln to plasma in the normal state; in the stressed state, this export is even greater. An amino acid transporter

* Corresponding author.
E-mail address: bilinsky@math.duke.edu (L.M. Bilinsky).

http://dx.doi.org/10.1016/j.jtbi.2015.04.006
0022-5193/

which may have an important role in Glu metabolism in a number of pathological states is the cystine/glutamate antiporter, which effects an obligate exchange of one hepatic Glu for one plasma cystine. This antiporter is not usually expressed in liver, but is induced during conditions of oxidative stress. Since Glu metabolism is complicated and central in dietary amino acid catabolism, GSH synthesis, and the TCA cycle, understanding how the liver and skeletal muscle work together to regulate its metabolism constitutes an important challenge.

A number of controversies surround Gln–Glu metabolism and the effects of amino acid supplementation in pathological states. Decreased plasma Gln levels are seen in acute catabolic states, in which there is an increased breakdown and decreased synthesis of skeletal muscle protein. Conditions accompanied by a catabolic state include sepsis, burns, trauma (including major surgery), uncontrolled diabetes, and starvation (Ardawi and Jamal, 1990). Droege and Holm (1997) have pointed out that a very large number of diseases and pathological conditions are characterized by both low plasma cystine and glutamine, often accompanied by many of the following: elevated plasma glutamate, increased urea production, low natural killer cell activity, and skeletal muscle wasting. These include late asymptotic stage HIV infection, sepsis, major injury and trauma, cancer, Crohn's disease, and ulcerative colitis. Droege et al. have termed this constellation of abnormalities "low CG syndrome." Although the net release of Gln from skeletal muscle into plasma is greatly increased during a catabolic state, increased demand by splanchnic and immunologic tissue (Cynober and Moore, 2003) results in depleted plasma Gln.

The depletion of plasma Gln has been found to be correlated with poor patient outcome, and there is evidence that supplementation with Gln improves outcome in cases including trauma and major surgery (Boelens et al., 2001), as well as burns (Garrel et al., 2003). In fact, it has been suggested (Watford, 2008) that Gln should be considered a conditionally essential amino acid. However, the mechanisms by which such supplementation improves patient condition are still not well understood. For example, Gln supplementation seems to help preserve muscle Gln concentration, usually depleted by about half, and it discourages the breakdown of muscle protein. Also not currently understood is how supplementation with *N* -acetylcysteine (NAC) causes a sturdy increase in plasma Gln levels in HIV patients (Droege and Holm, 1997).

Gln also plays a role in detoxification of exogenous toxins. Gln supplementation of rats undergoing acetaminophen (APAP) overdose acts to preserve GSH levels in liver and reduce the mortality rate relative to controls (Hong et al., 1992). During APAP overdose, the liver's ability to dispose of APAP is overwhelmed, causing it to be metabolized to the hepatotoxic compound NAPQI; NAPQI can be safely removed by conjugation with GSH but, during acute overdose, stores of GSH become depleted. The three amino acid precursors of GSH are cysteine (Cys), glutamate (Glu), and glycine (Gly) and under normal conditions cysteine is rate-limiting as it is present in the smallest concentration in hepatocytes. The results of Hong et al. (1992) suggest that during APAP overdose Glu can become rate-limiting for GSH formation; how this can occur is an interesting and important question.

In this paper we present a mathematical model of Glu–Gln metabolism in liver and skeletal muscle, and use it as a tool to investigate various physiological questions. Where possible, the model is based on information available for rat on amino acid transporter kinetics, the kinetics of biochemical reaction rates, etc. In the first section, we investigate the model's behavior for the case of normal physiologic conditions. We show that it reproduces precisely the empirically observed decline in liver GSH during starvation, as well as its diurnal variation under normal fed conditions. In the second section, we use the model to investigate changes resulting from a 9-day course of dexamethasone treatment. The alterations in amino acid uptake and release that occur in a catabolic state are believed to be mediated by glucocorticoids, potent anti-inflammatory hormones whose secretion into blood is upregulated during times of stress. Dexamethasone is a synthetic glucocorticoid and chronic dexamethasone administration has been used to study the metabolic changes characterizing a catabolic state, in isolation from the various pathologies causing the state (Ardawi and Jamal, 1990; Minet-Quinard et al., 2000). In the third section, we use the model to study APAP overdose and investigate the mechanism by which Gln preserves hepatic GSH levels.

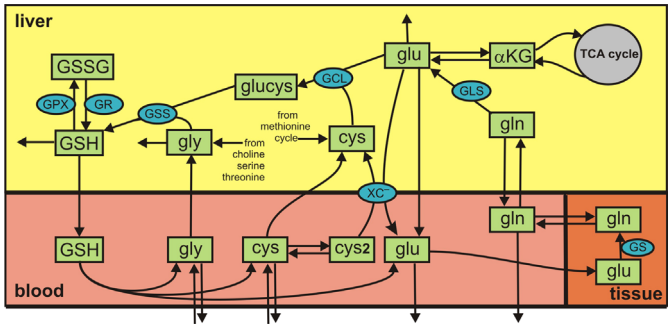

Fig. 1. Glu–Gln metabolism in liver and skeletal muscle tissue. Rectangles enclose the acronyms of substrates that are variables in the model. Arrows at the bottom of the figure represent import of dietary amino acids and import from other organs not explicitly modeled, and losses to organs not explicitly modeled as well as degradation. There is one differential equation for each substrate. The ellipses contain the acronyms of the enzymes that catalyze reactions. Full names for all substrates and a complete description of the mathematical model are given in the text. Full names for all enzymes and the values of all parameters are given in Tables 1–3.

2. Methods

Our model is a system of ordinary differential equations. The dependent variables represent the concentrations (in μM) of various substrates of interest (mainly amino acids and glutathione) in the liver, skeletal muscle, and blood plasma; these are represented by rectangular boxes in Fig. 1, which gives a schematic of the transport processes and biochemical reactions included in the model. Each differential equation is an expression of mass-balance: the time rate of change of a substrate concentration (in μM/h) is the sum of the velocities of reactions producing the substrate (and the velocity of transport into the compartment, where applicable), minus the sum of the velocities of reactions consuming the substrate (and the velocity of transport out of the compartment, where applicable). Enzymes catalyzing biochemical reactions are represented in Fig. 1 by blue ovals enclosing the enzyme's acronym.

The model we present here is a modification of the model for glutathione metabolism in Reed et al. (2008). The methionine and folate cycles are not explicitly featured and only cytosolic concentrations are considered; we do not track mitochondrial concentrations. However, we add the following new features: (1) the inclusion of glutamine as a substrate, (2) biochemical reactions producing and consuming glutamate in the liver, including a glutamate "pool" consisting of the TCA cycle intermediate α-ketoglutarate, and (3) the addition of a compartment for skeletal muscle. Although a large number of biochemical reactions occur in skeletal muscle, for our purposes it suffices to consider the concentrations of glutamate and glutamine there. We assume that the volume of liver (denoted by vL in the model) is 0.0054 L. We assume that the volume of skeletal muscle (vSM) is 0.1008 L and that the volume of blood plasma (vB) is 0.0108 L.

2.1. Determining model parameters

For both liver and skeletal muscle, uptake of a substrate from the blood plasma is assumed to obey Michaelis–Menten kinetics with K_m taken from the literature; the same holds for release of a substrate into blood plasma, although K_ms for efflux are often harder to find. When the K_m for efflux is not available, efflux is assumed to depend linearly on the cytosolic substrate concentration.

K_m values for enzymes and transporters can usually be found in the literature, but V_{max} values (in units relevant to our model, moles per unit time) are much harder to find as they are more difficult to measure and often depend on time-varying gene expression levels. Hence, V_{max} values are usually inferred. For example, where perfusion experiments were done that report the rate of uptake of a substrate by an organ at a given plasma concentration, this information was used to infer V_{max} for uptake of the substrate. In general, model parameters which could not be directly obtained from the literature were chosen so as to generate agreement between model solutions and published values for normal metabolite concentrations and (where available) reaction velocities, fluxes between organs and blood plasma, turnover rates in cytosol or blood plasma, etc.

In the following paragraphs we briefly review the differential equations associated with each compartment.

2.2. Liver

As in Reed et al. (2008), we model the import of cysteine from blood plasma and its production by the methionine cycle, and assume no release back into plasma. The methionine cycle is not modeled explicitly. Instead, we assume that it produces cysteine at the constant rate 100 μM/h. The differential equation for the concentration of liver cytosolic cysteine is

$$\frac{d[Cys]}{dt} = -V_{GCL}([\gamma GC],[Cys],[Glu],[GSH]) + 100 + \left(\frac{vB}{vL}\right)V_{cysin}([bCys]) - k_{l,cysloss}[Cys]^2 \quad (1)$$

The functional form for V_{GCL}, the velocity of the reaction by which cysteine and glutamate are combined to form γ-glutamyl–cysteine, is given in Reed et al. (2008). The dependence of V_{GCL} on gluthione concentration is due to the fact that GSH competes with glutamate in binding to glutamate–cysteine ligase (Richman and Meister, 1975; Seelig and Meister, 1985; Mendoza-Cozatl and Moreno-Sanchez, 2006). The quadratic removal term for cysteine from the cytosol captures loss to taurine synthesis and other pathways and follows Reed et al. (2008).

The differential equations for the concentration of liver cytosolic glutamate and α-ketoglutarate are

$$\frac{d[Glu]}{dt} = V_{GLS}([Gln]) - V_{GCL}([\gamma GC],[Cys],[Glu],[GSH]) - k_{ga}[Glu] + k_{ag}[\alpha KG] - V_{glutout}([Glu]) - k_{l,gluloss}[Glu] \quad (2)$$

$$\frac{d[\alpha KG]}{dt} = k_{ga}[Glu] - k_{ag}[\alpha KG] + k_{TCAin} - k_{TCAout}[\alpha KG] \quad (3)$$

Glutamate is generated from the hydrolysis of glutamine via the glutaminase reaction (GLS). We also model the exchange of Glu with α-ketoglutarate, a TCA-cycle intermediate which interconverts with Glu via transamination reactions. The flux through α-ketoglutarate due to the TCA cycle is assumed to be 19800 μM/h, obtained from studies on rats due to Jucker et al. (1998) and converted to our units. We note that there is no term for the uptake of glutamate from plasma. This is because there is strong evidence that only a tiny fraction of hepatocytes can take up vascular glutamate; these are the perivenous scavenger cells and constitute around 7% of hepatocytes (Kilberg and Haussinger, 1992). In our model we seek to describe the majority of hepatocytes and hence do not include glutamate import.

The three fates of cytosolic Glu in the model are consumption via the GCL reaction, export from the liver into the plasma, and a term which mainly reflects uptake by the glutamate-consuming perivenous scavenger cells. The perivenous scavenger cells are unique among hepatocytes in their expression of glutamine synthetase and their ability to consume glutamate; they scavenge ammonia molecules en route to the hepatic vein and combine them with glutamate to form glutamine, thus preventing them from entering the general circulation (Kilberg and Haussinger, 1992). Consistent with this role, we assume that some of the glutamate released by the periportal cells is taken up by the perivenous cells before entering the general circulation via the hepatic vein.

The differential equation for the concentration of liver glycine is

$$\frac{d[Gly]}{dt} = \left(\frac{vB}{vL}\right)V_{glyin}([bGly]) - V_{GSS}([Gly],[\gamma GC],[GSH]) + 19384.6 - k_{l,glyloss}[Gly] - k_{glyout}[Gly] \quad (4)$$

Converting values given in Wang et al. (2013) to our units, we assume that 19,385 μM/h of glycine is produced from choline, serine, and threonine and that an equal quantity is consumed by the synthesis of hippuric acid, heme, bile acids, and purines.

We model the transport of Gln between the blood plasma and liver, and the consumption of Gln by the glutaminase reaction. Rates of uptake and release of Gln by liver were estimated from Baird et al.'s studies with perfused rat liver (Baird et al., 2004).

$$\frac{d[Gln]}{dt} = \left(\frac{vB}{vL}\right)V_{glnin}([bGln]) - V_{GLS}([Gln]) - V_{glnout}([Gln]) \quad (5)$$

The differential equations for the concentrations of liver cytosolic GSH, GSSG, and γ-glutamyl-cysteine are

$$\frac{d[GSH]}{dt} = V_{GSS}([Gly],[\gamma GC],[GSH]) - V_{GSHlow}([GSH]) - V_{GSHhigh}([GSH]) - 2VGPX([GSH]) + 2VGR([GSSG]) - d[GSH] \quad (6)$$

$$\frac{d[GSSG]}{dt} = VGPX([GSH]) - VGR([GSSG]) - V_{GSSGlow}([GSSG]) - V_{GSSGhigh}([GSSG]) \quad (7)$$

$$\frac{d[\gamma GC]}{dt} = V_{GCL}([\gamma GC],[Cys],[Glu],[GSH]) - V_{GSS}([Gly],[\gamma GC],[GSH]) \quad (8)$$

We model the production of GSH from γ-glutamyl cysteine, its export from liver, and its interconversion with its oxidized counterpart, GSSG. In the interests of simplicity, the export of GSSG from liver is taken into account but its appearance in the blood plasma is not; the effect of its breakdown there is only a small correction to that of the breakdown of GSH since GSSG has concentration in plasma less than 0.5 μM (Reed et al., 2008).

2.3. Skeletal muscle

Our primary interest in skeletal muscle is its role as a source of glutamine for the liver. The differential equation for the concentration of glutamine in skeletal muscle is

$$\frac{d[smGln]}{dt} = \left(\frac{vB}{vSM}\right)V_{sm,glnin}([bGln]) - V_{sm,glnout}([smGln]) + V_{GS}([smGlu]) \quad (9)$$

We model the exchange of Gln between skeletal muscle and the blood plasma and note that there is a net efflux of glutamine from skeletal muscle under normal conditions. We model the synthesis

of Gln from Glu via glutamine synthetase (GS).

$$\frac{d[smGlu]}{dt} = \left(\frac{vB}{vSM}\right) V_{sm,glutin}([bGlu]) - V_{GS}([smGlu]) + p_{glu} \quad (10)$$

We assume based on the half-life of Glu in blood plasma (Klin et al., 2010) that the release of Glu from skeletal muscle into blood plasma is negligible. In addition to taking up Glu from the plasma, skeletal muscle takes up branched-chain amino acids in large quantity which can be converted to glutamate via transamination reactions. Asola et al. (2002) found that the uptake of amino acids by skeletal muscle in both fasting and insulin-clamped subjects was near 17 μM/(kg min), 1020 μM/h in our units. Branched-chain amino acids constitute about half of this uptake (Hutson et al., 2005). Since not all of this is converted to Glu, we choose $p_{glu} = 346.5$ μM/h for the rate at which Glu appears in skeletal muscle from this source.

2.4. Blood plasma

The differential equation for the concentration of glutamine in blood plasma is

$$\begin{aligned}\frac{d[bGln]}{dt} = & -V_{glnin}([bGln]) - V_{sm,glnin}([bGln]) \\ & + \left(\frac{vSM}{vB}\right) V_{sm,glnout}([smGln]) \\ & + \left(\frac{vL}{vB}\right) V_{glnout}([Gln]) - k_{p,glnloss}[bGln]\end{aligned} \quad (11)$$

We include a linear removal rate of glutamine from the plasma; this corresponds to absorption by tissues other than the liver, primarily the gut and kidney (Hensley et al., 2013).

The differential equation for the concentration of glutamate in blood plasma is

$$\begin{aligned}\frac{d[bGlu]}{dt} = & d_{deg}[bGSH] - V_{sm,glutin}([bGlu]) \\ & + \left(\frac{vL}{vB}\right) V_{glutout}([Glu]) - k_{p,gluloss}[bGlu]\end{aligned} \quad (12)$$

We assume no input to blood plasma of dietary glutamate or glutamine because these are largely utilized by the small intestine (Wu et al., 2004; Newsholme, 2001). Glutamate is generated in plasma by the breakdown of glutathione. In addition to the release of Glu from liver and uptake by skeletal muscle, there is a linear removal term capturing absorption by the gut and perivenous scavenger cells of the liver (Klin et al., 2010).

The equations governing the concentrations of glycine, cysteine, and cystine (Cys_2, the oxidized form of cysteine) in blood plasma are given below. Cysteine entering plasma is rapidly oxidized to cystine, and cystine can be reduced back to cysteine, largely by plasma GSH; we assume that as plasma GSH approaches 0, so does the rate of conversion of cystine to cysteine.

$$\begin{aligned}\frac{d[bGly]}{dt} = & d_{deg}[bGSH] + \left(\frac{vL}{vB}\right) V_{glyout}([Gly]) \\ & - V_{glyin}([bGly]) - k_{p,glyloss}[bGly] + glyin(t)\end{aligned} \quad (13)$$

$$\begin{aligned}\frac{d[bCys]}{dt} = & d_{deg}[bGSH] - V_{cysin}([bCys]) - k_{p,cysloss}[bCys] \\ & + 2\left(\frac{[bGSH]}{12.4}\right) k_{Cys2,Cys}[Cys_2] \\ & - 2k_{Cys,Cys2}[bCys] + cysin(t)\end{aligned} \quad (14)$$

Table 1
Transport parameters.

Description	Symbol	Parameter	Model value	References
μM/h				
Glu release from liver	$V_{glutout}$	V_{max}	1781	
		K_m	1200	Fork et al. (2011)
Gln uptake by liver	V_{glnin}	V_{max}	51,750	
		K_m	1700	Baird et al. (2004)
Gln release by liver	V_{glnout}	V_{max}	28,561	
		K_m	1700	Baird et al. (2004)
Cys uptake by liver	V_{cysin}	V_{max}	86,688	
		K_m	2100	Kilberg and Haussinger (1992)
Gly uptake by liver	V_{glyin}	V_{max}	15,537	
		K_m	150	Kilberg and Haussinger (1992)
low-affinity GSH transporter	V_{GSHlow}	V_{max}	943	
		K_m	3000	Inoue et al. (1984), Ookhtens and Maddatu (1991), and Ookhtens and Kaplowitz (1998)
high-affinity GSH transporter	$V_{GSHhigh}$	V_{max}	129	
		K_m	150	Inoue et al. (1984), Ookhtens and Maddatu (1991), and Ookhtens and Kaplowitz (1998)
low-affinity GSSG transporter	$V_{GSSGlow}$	V_{max}	25,261	
		K_m	7100	Inoue et al. (1984), Kondo et al. (1980), Ookhtens and Maddatu (1991), and Ookhtens and Kaplowitz (1998)
high-affinity GSSG transporter	$V_{GSSGhigh}$	V_{max}	1092	
		K_m	1250	Inoue et al. (1984), Kondo et al. (1980), Ookhtens and Maddatu (1991), and Ookhtens and Kaplowitz (1998)
Glu uptake by skeletal muscle	$V_{sm,glutin}$	V_{max}	9982	
		K_m	1050	Kilberg and Haussinger (1992)
Gln uptake by skeletal muscle	$V_{sm,glnin}$	V_{max}	154,295	
		K_m	9250	Kilberg and Haussinger (1992) and Hundal et al. (1991)
Gln release by skeletal muscle	$V_{sm,glnout}$	V_{max}	6290	
		K_m	9250	Kilberg and Haussinger (1992) and Hundal et al. (1991)

$$\frac{d[Cys_2]}{dt} = k_{Cys,Cys2}[bCys] - \left(\frac{[bGSH]}{12.4}\right) k_{Cys2,Cys}[Cys_2] \quad (15)$$

The differential equation for glutathione in blood plasma is

$$\frac{d[bGSH]}{dt} = \left(\frac{vL}{vB}\right) V_{GSHlow}([GSH]) + \left(\frac{vL}{vB}\right) V_{GSHhigh}([GSH]) - d_{loss}[bGSH] - d_{deg}[bGSH] + p_{gsh} \quad (16)$$

The low- and high-affinity GSH transporters in liver export approximately 450 μM/h GSH into the blood plasma. We assume that another $p_{gsh} = 450$ μM/h is released from skeletal muscle, consistent with studies in rats (Ookhtens et al., 1994; Kretzschmar, 1996) which found that skeletal muscle is responsible for about half of the GSH appearing in plasma. Since the efflux of GSH from muscle has been found to be relatively constant under conditions altering other aspects of muscle metabolism (Ookhtens et al., 1994; Kretzschmar, 1996), we do not model the concentration of GSH in skeletal muscle. The linear removal term for GSH reflects its breakdown into glutamate, cysteine, and glycine.

Table 1 gives parameter values for the amino acid and glutathione transporters included in the model. Except for the low-affinity GSH exporter in liver, transport velocities are assumed to be Michaelis–Menten in the substrate concentration. The low-affinity GSH exporter has the form given in (17). Liver glutaminase is confined to the mitochondria, where the concentration of glutamine is about 20,000 μM; the concentration in cytosol is about 7000 μM (Kilberg and Haussinger, 1992). Because we do not wish to introduce a mitochondrial compartment, we scale the true K_m by (7/20) so that the velocity of the glutaminase reaction can be computed from the cytosolic glutamine concentration.

Table 2 gives parameter values associated with the various biochemical reactions. Most reaction velocities are assumed to obey Michaelis–Menten kinetics; exceptions to this and the velocity of glutathione oxidation (which is Michaelis–Menten for two substrates because two GSH molecules are combined) are given in Eqs. (17)–(20). The motivation for these forms can be found in Reed et al. (2008). Table 3 gives the model values of parameters for which values are not available in the literature.

$$V_{GSHlow} = \frac{V_{max}[GSH]^3}{K_m^3 + [GSH]^3} \quad (17)$$

$$V_{GSS} = \frac{V_{max}\left([Gly][\gamma GC] - \frac{[GSH]}{K_e}\right)}{K_m^{\gamma GC}K_m^{gly} + [\gamma GC]K_m^{gly} + [Gly]K_m^{\gamma GC}\left(1 + \frac{[\gamma GC]}{K_m^{\gamma GC}} + \frac{[GSH]}{K_p}\right)} \quad (18)$$

Table 3
Other parameters.

Description	Parameter	Model value
h^{-1}		
Transamination of Glu to αKG	k_{ga}	0.37
Transamination of αKG to Glu	k_{ag}	1.89
Loss of αKG to TCA cycle	k_{TCAout}	15.8
Loss of liver Gly	$k_{l,glyloss}$	13.75
Loss of liver Glu	$k_{l,gluloss}$	0.23
Loss of liver GSH	d	0
Release of Gly from liver	k_{glyout}	12.38
Oxidation of plasma Cys to cystine	$k_{Cys,Cys2}$	13.85
Breakdown of plasma GSH	d_{deg}	54.44
Loss of plasma GSH	d_{loss}	18.15
Loss of plasma Cys	$k_{p,cysloss}$	27.08
Loss of plasma Gln	$k_{p,glnloss}$	3.49
Loss of plasma Glu	$k_{p,gluloss}$	5.57
Loss of plasma Gly	$k_{p,glyloss}$	2.35
$(h\ \mu M)^{-1}$		
Loss of liver Cys	$k_{l,cysloss}$	1.95
Reduction of plasma cystine to Cys	$k_{Cys2,Cys}$	3
μM/hr		
Production of α-KG from TCA cycle	k_{TCAin}	19,800
Production of plasma GSH from skeletal muscle	p_{gsh}	450
Production of Glu in skeletal muscle from BCAA	p_{glu}	346.5

Table 2
Biochemical reaction parameters.

Description	Symbol	Functional form	Parameter	Model value	References
μM/h					
Glutaminase in liver	V_{GLS}	MM	V_{max}	9648	
			K_m	9800 (see text)	Kilberg and Haussinger (1992)
Glutamate–cysteine ligase in liver	V_{GCL}	see Eq. (19)	V_{max}	3825	
			K_m^{cys}	100	Mendoza-Cozatl and Moreno-Sanchez (2006), Hell and Bergmann (1990), and Griffith (1999)
			K_m^{glu}	1900	Mendoza-Cozatl and Moreno-Sanchez (2006), Hell and Bergmann (1990), and Griffith (1999)
			K_e	5597	Mendoza-Cozatl and Moreno-Sanchez (2006), Hell and Bergmann (1990), and Griffith (1999)
			K_i	8200	Mendoza-Cozatl and Moreno-Sanchez (2006), Hell and Bergmann (1990), and Griffith (1999)
			K_p	300	Mendoza-Cozatl and Moreno-Sanchez (2006), Hell and Bergmann (1990), and Griffith (1999)
Glutathione synthetase in liver	V_{GSS}	see Eq. (18)	V_{max}	4149	
			$K_m^{\gamma GC}$	22	Mendoza-Cozatl and Moreno-Sanchez (2006) and Hell and Bergmann (1990)
			K_m^{gly}	300	Mendoza-Cozatl and Moreno-Sanchez (2006) and Hell and Bergmann (1990)
			K_e	5600	Mendoza-Cozatl and Moreno-Sanchez (2006) and Hell and Bergmann (1990)
			K_p	30	Mendoza-Cozatl and Moreno-Sanchez (2006) and Hell and Bergmann (1990)
Oxidation of GSH in liver	$VGPX$	see Eq. (20)	V_{max}	4809	
			K_m	1330	Carmagnol et al. (1983)
Reduction of GSSG in liver	VGR	MM	V_{max}	25,773	
			K_m	107	Latta and Augusteyn (1984) and Savvides et al. (2002)
Glutamine synthetase in skeletal muscle	V_{GS}	MM	V_{max}	1120	
			K_m	2470	Smith et al. (1984)

$$V_{GCL} = \frac{V_{max}\left([Cys][Glu] - \frac{[\gamma GC]}{K_e}\right)}{K_m^{cys}K_m^{glu} + K_m^{cys}[Glu] + K_m^{glu}[Cys]\left(1 + \frac{[GSH]}{K_i} + \frac{[Glu]}{K_m^{glu}}\right) + \frac{\gamma GC}{K_p} + \frac{[GSH]}{K_i}} \quad (19)$$

$$VGPX = V_{max}\left(\frac{[GSH]}{K_m + [GSH]}\right)^2 \quad (20)$$

3. Results I: the normal rat

3.1. Normal model steady-state concentrations and velocities

We view the rates at which dietary amino acids enter the blood plasma as the inputs to the model. In most simulations these are assumed to be constant in time and equal to the average hourly input over a day. We note that, due to metabolism by the gut, the rates at which amino acids enter blood plasma are not always equal to the dietary intake. The outputs computed by the model are the steady-state substrate concentrations and fluxes (velocities) in liver, blood plasma, and skeletal muscle obtained by solving the model differential equations. Although we usually use constant amino acid input rates, we can also investigate the model response to temporally varying inputs, as will be shown in the section on diurnal variation in liver GSH. In this case, the outputs are time-varying substrate concentrations.

We assume the following constant rates at which amino acids enter blood plasma: no input of glutamate or glutamine (see Methods section), a Cys input of 210 μM/h, and a Gly input of 370 μM/h. Within the liver, Cys is assumed to be generated at rate 100 μM/h by the methionine cycle. Table 4 shows the steady-state substrate concentrations and fluxes computed by the model for these inputs. Fluxes of form V_{bXl} denote the net uptake of substrate X from blood plasma by the liver. Fluxes of form V_{bXSM} denote the net uptake by skeletal muscle. Negative values indicate a net release. V_{lGSHb} and V_{lGSSGb} denote the total release of GSH and GSSG from liver into blood plasma via both the low and high affinity transporters. The model reproduces well the experimentally determined values for these quantities available in the literature; where necessary, the published values have been converted to our units (μM or μM/h).

3.2. The half-life of glutathione

Cytosolic GSH in rat liver has a half-life of 2–3 h (Lu, 1999). This figure refers to the time it takes for GSH to decline under conditions in which its new formation is blocked, such as by treatment with an agent which inhibits GCL (the enzyme catalyzing the first step in GSH synthesis); see for example experiments due to Ookhtens et al. (1985). Fig. 2 shows the time course of total liver glutathione (GSH + 2 GSSG) computed by the model when V_{max} for the GCL reaction is set to 0. The model predicts a half-life of about 3 h, consistent with experimental findings.

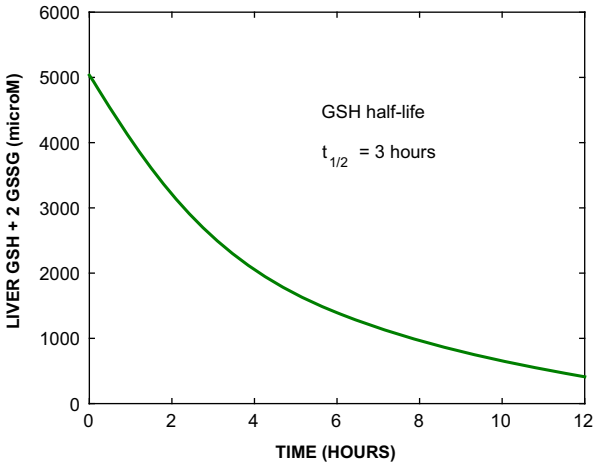

Fig. 2. GSH half life after GCL is blocked. When GSH synthesis is stopped the model intracellular GSH concentration declines rapidly with a half-life of approximately 3 h, consistent with experimental findings (Lu, 1999).

Table 4
Normal rat concentrations and velocities.

Conc. (μM)	Range/comment	Source	Velocity (μM/h)	Range/comment	Source
Liver					
GSH = 4996	4950–5310	Ookhtens et al. (1985)	$V_{GCL} = 1050$		
γ-GC	9.8				
GSSG = 17	≈ 1/300 GSH conc.	Moslen and Smith (1992)	$V_{GSS} = 1050$	≈ GSH + 2 GSSG efflux	Lauterburg et al. (1984)
Glu = 6401	6400	Haussinger et al. (1985)	$VGPX = 5999$	1200–6000	Hillesheim et al. (1995)
Cys = 60	20–100	Stipanuk et al. (2006)	$VGR = 5849$		
Gly = 1410	1230–1590	Scheer et al. (2005)	$V_{GLS} = 4019$	3840–4140	Haussinger (1986)
Gln = 6997	7000	Kilberg and Haussinger (1992)	$V_{TCAin} = 19800$		Jucker et al. (1998)
αKG = 1253	1230	Siess et al. (1977)	$V_{TCAout} = 19800$	Flux through αKG from TCA cycle	Jucker et al. (1998)
			$V_{Glu \to \alpha KG} = 2368$		Friday et al. (2012)
			$V_{\alpha KG \to Glu} = 2368$	No net flux between *Glu* and αKG	Friday et al. (2012)
Skeletal muscle					
Glu = 1596	1380–1812	Leweling et al. (1996)	$V_{GS} = 439$		
Gln = 2762	2506–3020	Leweling et al. (1996)			
Blood plasma					
Glu = 100	103.7–190.9	Muratsubaki and Yamaki (2011)	$V_{bCysl} = 1066$		
Gln = 600	≈ 600	Kilberg and Haussinger (1992)	$V_{bGlnl} = 4019$		
Cys = 13	8–40	Bannai (1984) and Stipanuk et al. (2006)	$V_{bGlyl} = 1050$		
Gly = 221	210.9–249.9	Muratsubaki and Yamaki (2011)	$V_{bGlul} = -1500$	−1200 to −1800	Haussinger et al. (1989)
$Cys_2 = 60$	32–90	Bannai (1984) and Stipanuk et al. (2006)	$V_{lGSHb} = 900$	906–1014	Ookhtens et al. (1985)
GSH = 12.4	11.42–13.38	Ookhtens et al. (1994)	$V_{lGSSGb} = 75$	60–120	Bartoli and Sies (1978)
			$V_{bGluSM} = 93$		
			$V_{bGlnSM} = -439$		
			$cysin = 210$		
			$glyin = 370$		

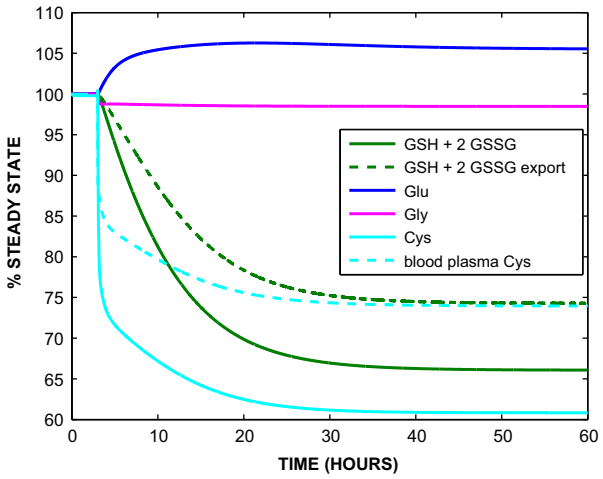

Fig. 3. GSH and GSH transport under fasting conditions. After 3 h, the inputs of cysteine, glycine, and the production of cysteine from the methionine cycle in liver are reduced to 1/3 of normal, mimicking a fasting condition. The total intracellular glutathione concentration (GSH+2 GSSG) computed by the model declines to about 65% its normal value, in good agreement with Aw et al. (1986) as well as Tateishi et al. (1974). The rate of glutathione export declines to about 75% its usual value, consistent with the findings of Aw et al. (1986). Liver Cys declines sharply and parallels the decline in plasma Cys.

The decline of liver GSH in response to fasting is much more gradual than would be expected from the half-life; experiments by Aw et al. (1986) on fasted rats found that after 48 h, liver GSH was only reduced by 44%. During starvation there is an increased breakdown of skeletal muscle protein which partially compensates for the absence of dietary input of amino acids, but this effect is not large enough to explain the data. A possible explanation, proposed by Reed et al. (2008), is that most of the cysteine, glycine, and glutamate exported from liver in the form of GSH is released into the plasma by its breakdown and then reabsorbed by the liver. Under this scenario, dietary input of amino acids serves largely to replenish net loss of cysteine, glutamate, and glycine to processes not associated with glutathione. We note that in our model we assume no dietary input of Glu to blood plasma, as dietary Glu is almost completely utilized by the small intestine (Wu et al., 2004). In our model, Glu is produced from Gln via the GLS reaction in liver and skeletal muscle.

Fig. 3 shows the time course of liver cytosolic glutathione, expressed as a percentage of its normal value, computed by the model in response to a 48 h fast beginning at $t=3$. To simulate amino acid release from protein breakdown, all amino acid inputs (including the generation of cysteine from the methionine cycle in liver) are set equal to 1/3 their usual values during the fast. The model predicts that 48 h of fasting reduces liver glutathione to about 60% its normal value, in good agreement with Aw et al. (1986) as well as Tateishi et al. (1974). Also plotted are the time courses for the rate of glutathione export from liver, the cytosolic and blood plasma concentrations of Cys, and the cytosolic concentrations of Gly and Glu. The model predicts a reduction in the export rate of glutathione to about 67% its usual value, consistent with the findings of Aw et al. (1986), and a precipitous decline in cytosolic and plasma Cys. The decline in liver GSH parallels that of Cys and occurs despite the fact that liver Gly and Glu are near their normal values (recall that Gly and Glu are present in much greater concentration than Cys in the liver). This supports the view that Cys is rate-limiting for GSH production. Clear evidence for this was provided by Jaeschke and Wendel (1985), who showed that GSH levels in 48-h fasted mice rebounded to normal levels within 2 h of I.V. injection of 0.5 mmole per kg *N*-acetylcysteine. Our model reproduces this rebound very well; see Fig. 4.

3.3. Diurnal variation in liver glutathione

In the same work, Jaeschke discovered a diurnal variation in mouse liver glutathione content. For the time points considered (10 a.m., 2 p.m., 6 p.m., 2 a.m. and 6 a.m.) glutathione rose from 6 p.m. to 6 a.m. and declined from 10 a.m. to 6 p.m. Glutathione content in kidney, spleen, and lung was also studied and no such diurnal variation seen, suggesting that the effect was due to the nocturnal feeding of the mice. Reversal of the feeding schedule by restricting feeding to 7 a.m.–5 p.m. reversed the diurnal pattern, confirming this.

We model the mice's nocturnal feeding schedule by assuming that all amino acid inputs alternate between 200% of the mean hourly input over a day (from $t=0$ to $t=12$, corresponding to 8 p.m.–8 a.m.) and 0 (from $t=12$ to $t=24$, corresponding to 8 a.m.–8 p.m.). The computed glutathione concentration did show the

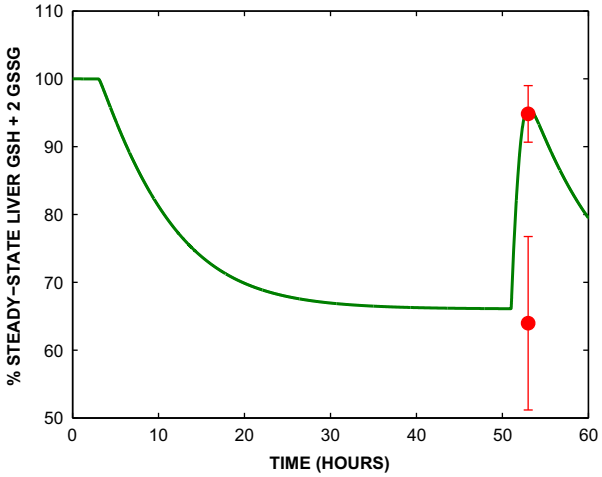

Fig. 4. NAC injection returns liver GSH to normal levels after a 48-h fast. After a 48-h fast, corresponding to $t=51$, a quantity of Cys is given over the course of a tenth of an hour equivalent to 0.5 mmol per kg. Glutathione (GSH + 2 GSSG) concentration computed by the model rebounds to normal levels within 2 h, consistent with data (shown in red) collected in experiments by Jaeschke and Wendel (1985). Also consistent with Jaeschke is the finding that most of the decrease in hepatic glutathione occurred within the first 24 h.

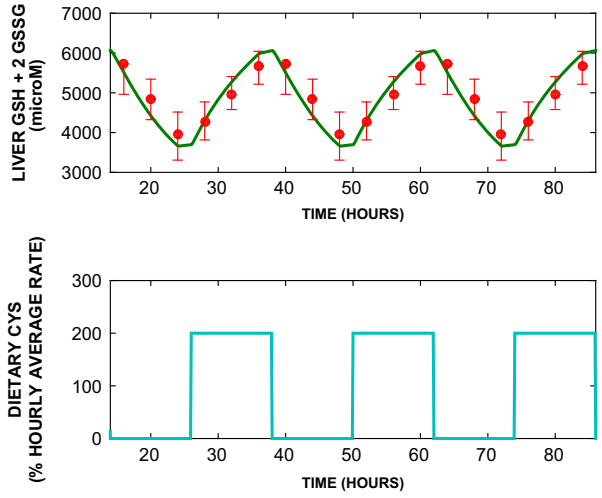

Fig. 5. Diurnal variation in liver glutathione. Plasma Cys input and production from the methionine cycle was set to be zero for a 12-h period from 8 a.m. to 8 p.m. ($t=26$ corresponds to 8 p.m. in the figure) and twice the uniform hourly input rate used elsewhere in this paper over a 12-h period from 8 p.m. to 8 a.m. The input of Gly was held constant at its usual value. The diurnal variation in liver glutathione computed by the model (green curve) is in excellent agreement with data (shown in red) collected in experiments by Jaeschke et al. for mice (Jaeschke and Wendel, 1985).

diurnal variation found by Jaeschke et al. In fact, to reproduce the diurnal variation it was sufficient to use a constant input for Gly and only alternate the Cys inputs (See Fig. 5. Green curve in top panel is liver glutathione computed in response to the alternating Cys input shown in the bottom panel; input from the methionine cycle was also assumed to alternate. Glutathione concentration in mouse liver is somewhat higher than in rat and the computed glutathione concentration was scaled to reflect this.). This lends further support to the idea that under normal or starved conditions, Cys concentration in the liver dictates the concentration of glutathione.

4. Results II: the glucocorticoid-treated rat

4.1. Modification of model

4.1.1. Dexamethasone

To simulate daily administration of dexamethasone, we introduced a parameter g to represent dexamethasone concentration in tissue and modeled it as increasing monotonically from 0 to a steady state of 1 after 9 days, consistent with its half-life of about 48 h; see Eq. (21). We note that the week-long period over which dexamethasone concentration rises is longer than the time scale on which dexamethasone induces changes in amino acid transport and enzyme regulation. For example, V_{max} and K_m for glutamine uptake by skeletal muscle stabilized at new values within 2 h of perfusion at a fixed dexamethasone concentration (Hundal et al., 1991). Hence, we used a quasi-static approximation, in which transport parameters and enzyme activities modulated by dexamethasone were taken to instantaneously stabilize at values determined by the current concentration of dexamethasone. For example, V_{max} for glutamine uptake by skeletal muscle was viewed as a linear function of g, where $V_{max}(0)$ is the maximal transport velocity for control rats while $V_{max}(1)$ is the maximal transport velocity for muscle perfused with 200 nM dexamethasone (represented by $g=1$ in our model), about 2/3 smaller. For simplicity, all parameters impacted by dexamethasone were viewed as linear functions of g.

$$\frac{dg}{dt}=\frac{\ln(2)}{48}(1-g) \tag{21}$$

Another modulatory hormone which is found to be present at elevated concentrations during chronic dexamethasone administration is insulin; Ardawi found that insulin levels were approximately 160% larger than normal.

4.1.2. Liver

In keeping with findings due to Gebhardt and Kleemann (1987) and Low et al. (1992) that the combination of dexamethasone and insulin effect an increase in the V_{max} for glutamine uptake by liver, we assume an increase in V_{max} of about 40%. Hepatic glutaminase expression has been found to be strongly upregulated by dexamethasone (Chung-Bok et al., 1997), and we assume an increase in V_{max} for the GLS reaction of 120%. Allan and Titheradge (1984) found that the rate of gluconeogenesis was nearly doubled in hepatocytes isolated from rats treated with dexamethasone relative to controls; hence we assume that dexamethasone causes an increased consumption of α-ketoglutarate by the TCA cycle.

4.1.3. Skeletal muscle

We assume that V_{max} and K_m for glutamine uptake by skeletal muscle change in response to dexamethasone as found by experiments due to Hundal et al. (1991). No analogous experiments were done for glutamine release, but as both uptake and release from skeletal muscle are mediated by the same amino acid transport system (system N_m) we assume K_m for release is altered in approximately the same way and chose V_{max} for efflux according to balance considerations.

We assume that dexamethasone increases V_{max} for the GS reaction by 165%, similar to the increase observed by Ardawi in the rate of glutamine synthesis by rat hindlimb (Ardawi and Jamal, 1990).

We assume that p_{glu} is increased by 185% in DEX rats due to increased production of glutamate from branched-chain amino acids (BCAAs) released during the breakdown of skeletal muscle protein; we also subsume under this term glutamate that is released during protein breakdown. BCAAs contribute to the generation of Glu in two ways: they can undergo transamination with α-ketoglutarate to generate glutamate, and their carbon skeletons can be converted to α-ketoglurate via catabolism in the TCA cycle. Ardawi found that in DEX rats α-ketoglutarate in skeletal muscle was half its usual value, consistent with the idea that these reactions generate much of the Glu used to synthesize Gln during DEX treatment. We assume that the release of Gln from protein breakdown is negligible compared to its production by the GS reaction (Ardawi and Jamal, 1990).

4.1.4. Blood plasma

In light of findings due to Gebhardt and Mecke (1983) showing dramatically increased uptake of Glu by rat hepatocytes treated with dexamethasone, we assume that dexamethasone effects a significant increase in the uptake of Glu by the perivenous scavenger cells of the liver (the tiny fraction of hepatocytes which take up vascular Glu). We do not explicitly model these cells but view their uptake as loss of Glu to tissues other than the skeletal muscle, and assume that it is approximately 225% larger in DEX rats relative to controls. One of the features of catabolic illness in humans is an increased uptake of glutamine by the small intestine (Cynober and Moore, 2003), and Ardawi et al. found that enterocytes isolated from the small intestine of dexamethasone-treated

Table 5
Modified parameters: dexamethasone treatment.

Description	Symbol	Parameter	Model value
μM/h			
Glutaminase in liver	V_{GLS}	V_{max}	9648 (1+1.2g)
Loss of αKG to TCA cycle		k_{TCAout}	15.8 (1+3g)
Gln uptake by liver	V_{glnin}	V_{max}	51,750 (1+0.39g)
Loss of plasma Gln		$k_{p,glnloss}$	3.49 (1+1.5g)
Loss of plasma Glu		$k_{p,gluloss}$	5.57 (1+2.268g)
Glu uptake by skeletal muscle	$V_{sm,glutin}$	V_{max}	9982 (1−0.77g)
Gln uptake by skeletal muscle	$V_{sm,glnin}$	V_{max}	154,295 (1−(2/3)g)
		K_m	9250 (1−0.77g)
Gln release from skeletal muscle	$V_{sm,glnout}$	V_{max}	6290 (1−0.332g)
		K_m	9250 (1−0.85g)
Glutamine synthetase in skeletal muscle	V_{GS}	V_{max}	1120 (1+1.65g)
Production of Glu in skeletal muscle from BCAA		p_{glu}	346.5 (1+1.85g)

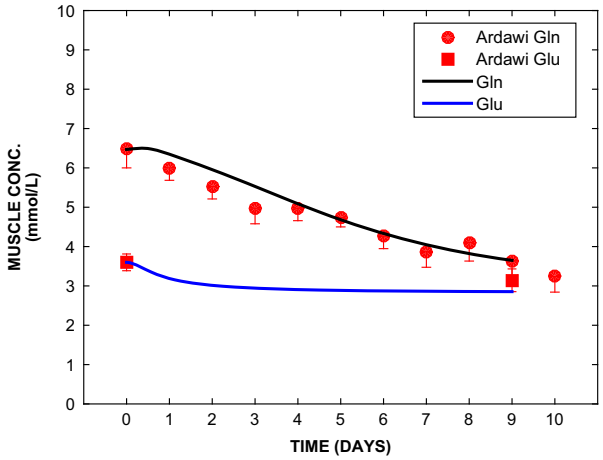

Fig. 6. Linear decline in intramuscular Gln with dexamethasone administration. The concentration of Gln computed by the model declines approximately linearly with time over a 9-day course of dexamethasone injection, in excellent agreement with data (shown in red) collected by Ardawi and Jamal (1990); injections were discontinued after 9 days but a final data point was collected for day 10. Also shown is the Glu concentration computed by the model, compared with Ardawi's data on Glu concentration in a control group of rats (plotted for day 0) and in a group given 9 days of dexamethasone injections (plotted for day 9). The model predictions correspond well to the data.

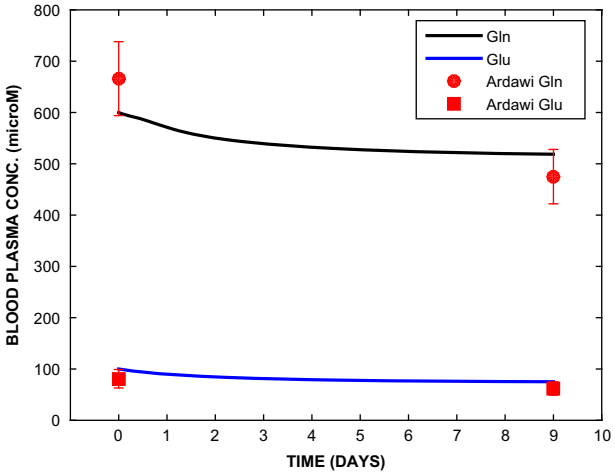

Fig. 7. Decline in plasma Gln and Glu with dexamethasone administration. The concentrations of Gln and Glu in plasma computed by the model decline over the 9 days of dexamethasone administration, and are in agreement with data collected by Ardawi et al. for control rats (plotted for day 0) and dexamethasone-treated rats (plotted for day 9).

rats had an increased rate of utilization of glutamine relative to controls (Ardawi et al., 1988). In the model we assume the loss of glutamine from blood plasma to tissues other than liver and skeletal muscle is about 150% larger in DEX rats than in controls.

Table 5 summarizes the model parameter dependencies on dexamethasone.

4.2. Simulation of dexamethasone experiments

4.2.1. Linear decline in muscle Gln concentration

Fig. 6 replots data taken from Fig. 1 of Ardawi and Jamal (1990), which gives the muscle intracellular Gln concentration on each day of the 10-day experiment; DEX was given for 9 days (injections on days 0–8) but a data point was taken for day 10. Overlayed onto their data is the time course of Gln as calculated by our model, where we have scaled the Gln concentration so that 2763 μM, our assumed normal cytosolic Gln concentration, corresponds to 6.47 mM, the concentration of Gln on day 0 as measured by Ardawi. We note that their figure includes Gln in the mitochondria, where it is at higher concentration than in the cytosol. Our model reproduces well the linear decline to a concentration about half the starting value. We note that although the last injection was given on day 8, the long half-life of dexamethasone is responsible for the continued decline between days 9 and 10. Consistent with Ardawi, Hundal et al. (1991) found that DEX administration resulted in a muscle intracellular concentration depleted by about half relative to controls (7.3 ± 0.50 mM in controls versus 3.9 ± 0.60 mM in DEX rats).

Also plotted is the (scaled) time course of Glu in muscle predicted by the model and two data points collected by Ardawi; the data point plotted for day 0 is the concentration of Glu in the skeletal muscle of controls and the data point plotted for day 9 is the concentration in DEX rats after 9 days of injections. Our model reproduces this slight but significant ($P < 0.05$) depletion of intramuscular Glu.

Our model reproduces other experimental findings as well. Ardawi measured the net efflux of Gln from skeletal muscle using arteriovenous concentration differences and found that 9 days of dexamethasone injections increased the net Gln efflux by about 150% relative to controls. Hundal measured net Gln efflux in controls versus DEX rats and obtained similar results. Our model is consistent with these findings. Hundal also measured net uptake of Glu by skeletal muscle and found that it is reduced by approximately 80% in DEX rats relative to controls; our model reproduces this.

4.2.2. Decline in plasma Gln and Glu concentrations

Fig. 7 plots the model solutions for plasma Gln and Glu over the course of the experiment and compares them with measurements made by Ardawi of Gln and Glu in the plasma of controls (plotted for day 0) and DEX rats after 9 days of injections (plotted for day 9). The model reproduces the statistically significant drop in plasma Gln and Glu caused by dexamethasone.

4.2.3. Gln and Glu concentrations in liver

Fig. 8 shows the time courses of Gln, Glu, α-ketoglutarate and GSH concentrations in liver as computed by the model. Low et al. (1992) found no significant change in the concentration of liver Gln in DEX rats relative to controls, but did find that liver Glu was greatly increased. The doubling of liver Glu concentration after 9 days of DEX treatment computed by the model is consistent with their data.

4.3. Induction of catabolic-state metabolism by dexamethasone

A major question which motivated Hundal's investigation of the effect of dexamethasone on Gln transport in skeletal muscle is how to reconcile the following three effects of dexamethasone on skeletal muscle Gln metabolism: (i) an increase in the flux through the GS reaction, (ii) a dramatic fall in intramuscular Gln, and (iii) a dramatic increase in the net efflux of Gln from muscle even though the Gln gradient of intramuscular to plasma Gln is decreased. They hypothesized that dexamethasone must alter Gln transport and found that it effects a dramatic reduction in both V_{max} and K_m.

Our model simulations demonstrate that the dexamethasone-induced changes in V_{max} and K_m for Gln transport in muscle are sufficient to explain how a greatly increased net efflux of Gln can be sustained even while intramuscular Gln levels fall. The large reduction in K_m (by about 75%) causes the net efflux to be approximately constant even while intramuscular Gln falls to half its normal value; this is why the model reproduces the linear decline in intramuscular Gln over 9 days of DEX administration found by Ardawi.

The upregulation of flux through the GS reaction found in DEX rats by Ardawi and Max was necessary to account for the increased net efflux of Gln; the decrease in intramuscular Gln, although dramatic, was not sufficient. Ardawi found that 9 days of dexamethasone administration only reduced intramuscular Glu by

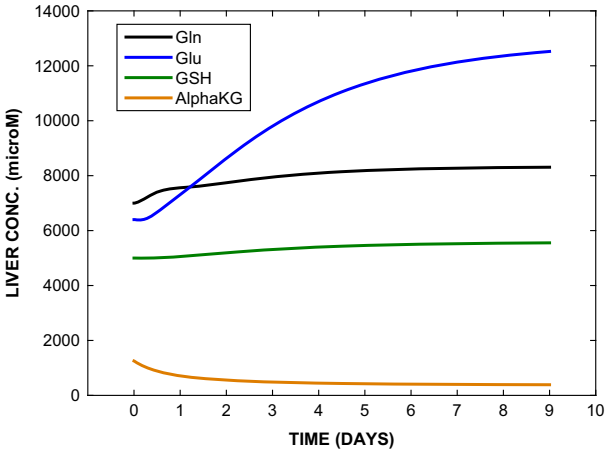

Fig. 8. Time course of substrate concentrations in liver with dexamethasone adminstration. Shown are the time courses of various substrates in liver computed by the model over 9 days of dexamethasone administration. Glu concentration approximately doubles, consistent with experimental findings of Low et al. (1992).

around 10%. Since Glu levels in muscle are held approximately constant, the flux through the GS reaction is as well. Hence, we have the interesting finding that dexamethasone administration results in a situation in skeletal muscle in which the rates of net Gln release and Gln synthesis are constant and enhanced, while the intramuscular Gln concentration declines dramatically.

Our model predicts no significant change in liver Gln concentration, but elevated levels of Glu in response to dexamethasone administration, consistent with a scenario of increased gluconeogenesis. Glucocorticoid levels are elevated during catabolic states (such as starvation), which are characterized by enhanced gluconeogenesis in splanchnic organs at the expense of skeletal muscle protein. Our model synthesizes what is known about the quantitative changes effected by dexamethasone on relevant transport rates and reaction velocities in liver and skeletal muscle, and explains how they can mediate the conversion of amino acids in skeletal muscle to glucose in the liver. We now summarize this process.

Glucocorticoids stimulate muscle protein breakdown. This liberates some small amount of glutamine, but much more is produced in muscle via the upregulated GS reaction, ultimately from BCAAs and α-ketoglutarate. This Gln is released in large quantity into the plasma by muscle due to the action of glucocorticoids on the Gln transporter. The liver then takes up Gln at an enhanced rate. Once in the liver, the upregulation in liver GLS transforms most of this Gln to Glu; the increased concentration of Glu drives formation of the TCA-cycle intermediate α-ketoglutarate from which glucose can be synthesized. Our concern here is Gln, but we note that the other substrate liver can use to form glucose is alanine, also released from skeletal muscle. Hence, the various changes in substrate concentrations in muscle, blood plasma, and liver seen during DEX administration are consistent with the production of glucose at the expense of muscle protein. This supports the idea that glucocorticoids are responsible for inducing the alterations in metabolism characterizing the catabolic state.

5. Results III: APAP overdose in the rat

Overdose of acetaminophen (APAP) results in the formation in liver of NAPQI, a compound toxic to liver cells; most NAPQI is formed in the endoplasmic reticulum by P450 enzymes. NAPQI can only be removed by conjugation with glutathione, and during APAP overdose glutathione levels become extremely depleted. Of the three amino acid precursors of glutathione (cysteine, glutamate, and glycine), cysteine has the lowest concentration in liver cells and is therefore considered rate-limiting. Current rescue protocols for acute APAP overdose focus on increasing liver cysteine, via I.V. infusion of *N*-acetylcysteine.

NAPQI which is not removed by GSH binds to mitochondrial proteins in hepatocytes, inducing necrosis and triggering an inflammatory response (Jaeschke et al., 2012) which has been referred to as "sterile inflammation." In experiments in mice, 1–2 h after APAP overdose Kupffer cells (the resident macrophages of the liver) release cytokines. The inflammatory cytokines result in the recruitment of neutrophils to liver which remove necrotic cell debris, and evidence suggests that this inflammatory response is primarily beneficial (Jaeschke et al., 2012). We note that immunologic cells are great consumers of Gln (Newsholme, 2001) and this results in the dramatic drop in plasma Gln seen during catabolic illness (Cynober and Moore, 2003).

5.1. Modification of model

5.1.1. Cortisol

We hypothesize for two reasons that cortisol levels rise at the start of the inflammatory process. First, cortisol rapidly triggers glutamine release from skeletal muscle, consistent with the sharp rise in plasma Gln within the first 6 h of APAP overdose in Hong's rats. Second, cortisol production is sometimes triggered at the start of an inflammatory process in order to keep it under control. In these simulations we take the variable *g*, which represented dexamethasone in the last section, to represent cortisol levels in excess of baseline. *g* evolves according to Eq. (22) where *dexon* is a variable equal to 1 when $2 \le t \le 13$ and 0 otherwise. This results in the following behavior: *g* begins to increase from 0 at $t=2$ h after overdose, nearly attains the steady-state value of 1 by about $t=5$, and begins decaying at $t=13$; studies of the sterile inflammatory process in mice undergoing APAP overdose found that the accumulation of neutrophils in mouse liver had reached its maximal value by the 13-h mark (Lawson et al., 2000).

$$\frac{dg}{dt} = 0.9(dexon - g) \tag{22}$$

5.1.2. Cystine–glutamate antiporter

Under normal circumstances, the liver can import cysteine but not cystine (the oxidized form) from blood plasma. However, Bannai et al. (1986) found that culturing hepatocytes with various electrophilic agents resulted in the induction of the cystine–glutamate transporter, also known as system Xc^-. This transporter effects an obligate exchange of cystine for glutamate: one cystine molecule in the blood plasma is pulled in and one intracellular glutamate is pushed out. Once inside the hepatocyte, the cystine is rapidly reduced to two cysteine molecules and incorporated into glutathione. As NAPQI is also an electrophilic agent, we speculate that it also induces system Xc^-. Insulin and dexamethasone also induce this transporter with a delay of about 12 h (Lu, 1999), and in studies of APAP overdose in mice, Hinson et al. found that blood insulin levels increased dramatically after APAP overdose, reaching 300% the normal concentration at 3 h after overdose, 1100% at 8 h, and 800% at 24 h (Hinson et al., 1984).

No published functional forms for the cystine–glutamate antiporter exist, so we choose a reasonable, simple functional form for the antiporter somewhat similar to forms that have been used for other antiporters in the literature (Keener and Sneyd, 2009); see Eq. (23). Here, $[Glu]$ is the cytosolic glutamate concentration in liver and $[Cys_2]$ is the cystine concentration in blood plasma. The four differential equations modified by inclusion of the antiporter are given below. The variable x_c^- models the induction time for the antiporter; see Table 6. The term *cys2in* appearing in the equation for cystine is explained below in the section on blood plasma. We note that the rate at which plasma cystine is reduced to cysteine

Table 6
Modified parameters: APAP overdose.

Description	Symbol	Parameter	Model value
Expression level of cystine–glutamate antiporter		x_c^-	0 for $0<t<3$ $\frac{t-3}{t-2}$ for $t\geq 3$
μM/hr			
Glu uptake by skeletal muscle	$V_{sm,glutin}$	V_{max}	$9982\ (1-0.77g)$
Gln uptake by skeletal muscle	$V_{sm,glnin}$	V_{max}	$154{,}295\ (1-(2/3)g)$
		K_m	$9250\ (1-0.77g)$
Gln release from skeletal muscle	$V_{sm,glnout}$	V_{max}	$6290\ (1-0.332g)$
		K_m	$9250\ (1-0.6545g)$
Glutamine synthetase in skeletal muscle	V_{GS}	V_{max}	$1120\ (1+u)$
Cys_2 appearing in plasma from fibrillin	$cys2in$		0 for $0<t<2.5$ $3333\ \frac{(t-2.5)^2}{(t-2.5)^2+1}$ for $2.5\leq t<7.5$ $3333\ e^{-0.8(t-7.5)}$ for $t\geq 7.5$
GCL flux in liver	V_{GCL}	V_{max}	3825 for $0<t<2$ $3825\ \left(1+0.6\left(\frac{t-2}{t+2}\right)\right)$ for $t\geq 2$
h^{-1}			
Consumption of GSH in liver		d	$1.2\ \left(\frac{t}{t+1}\right)$ for $0<t<6$ $1.2\ e^{-1.3(t-6)}$ for $t\geq 6$
Transport of cytosolic Gln into mitochondria		$k_{Gln,cm}$	1
Transport of mitochondrial Gln into cytosol		$k_{Gln,mc}$	0.2835
Loss of plasma Gln		$k_{p,glnloss}$	3.49 for $0<t<6$ $3.49\ (1+4.5g\ \frac{(t-6)^2}{(t-6)^2+1})$ for $t\geq 6$
Loss of plasma Glu		$k_{p,gluloss}$	$5.57\ (1+2.268g)$

must saturate with increasing cystine concentration due to a limited concentration of substances such as GSH which can effect this reduction. This is an important effect to model in this section as a large quantity of cystine is entering plasma.

$$V_{Cys2/Glu}([Cys_2],[Glu]) = 1000[Glu]\frac{[Cys_2]}{[Cys_2]+25} \tag{23}$$

$$\frac{d[Glu]}{dt} = V_{GLS}([Gln]) - V_{GCL}([\gamma GC],[Cys],[Glu],[GSH]) - k_{ga}[Glu] + k_{ag}[\alpha KG] - x_c^- V_{Cys2/Glu}([Cys_2],[Glu]) - V_{glutout}([Glu]) - k_{l,gluloss}[Glu] \tag{24}$$

$$\frac{d[Cys]}{dt} = -V_{GCL}([\gamma GC],[Cys],[Glu],[GSH]) + 100 + \left(\frac{vB}{vL}\right)V_{cysin}([bCys]) - k_{l,cysloss}[Cys]^2 + 2x_c^- V_{Cys2/Glu}([Cys_2],[Glu]) \tag{25}$$

$$\frac{d[bGlu]}{dt} = d_{deg}[bGSH] - V_{sm,glutin}([bGlu]) + \left(\frac{vL}{vB}\right)V_{glutout}([Glu]) - k_{p,gluloss}[bGlu] + x_c^- V_{Cys2/Glu}([Cys_2],[Glu]) \tag{26}$$

$$\frac{d[Cys_2]}{dt} = k_{Cys,Cys2}[bCys] - 120\left(\frac{[bGSH]}{12.4}\right)k_{Cys2,Cys}\frac{[Cys_2]}{[Cys_2]+60} - x_c^- V_{Cys2/Glu}([Cys_2],[Glu]) + cys2in(t) \tag{27}$$

5.1.3. Liver

In addition to the induction of the cystine–glutamate antiporter, we model APAP overdose as effecting a number of other changes in liver metabolism. We do not explicitly model the concentration of NAPQI in liver, but assume that it causes GSH to be consumed at a rate linear in GSH concentration and with time-varying rate coefficient equal to 0 at $t=0$ and saturating to 1.2 before $t=6$ h. At $t=6$ h, the rate coefficient beings to decay exponentially to reflect the fact that NAPQI is on the decline.

Lu et al. (1992) found that culturing hepatocytes with insulin and cortisol resulted in an increase of 45–65% in the activity of glutamate–cysteine ligase; V_{max} was altered but K_m was not. The earliest significant change occurred at 4 h. No change in glutathione synthetase activity occurred. We assume a sigmoidal increase with respect to time in V_{max} for glutamate–cysteine ligase from its baseline value to an asymptotically-approached maximal value that is 160% the baseline value. We assume the increase begins $t=2$ h after APAP overdose (when cortisol levels begin to rise), with half-maximum achieved 4 h later, and that enzyme activity remains elevated for the 24-h period considered.

We assume the normal value of V_{max} for glutamine uptake over the course of APAP overdose, because its hormonally induced upregulation takes 18–30 h to occur (Gebhardt and Kleemann, 1987). We assume the normal value of V_{max} for the GLS reaction because plasma insulin levels are tremendously increased during APAP overdose and Elgadi et al. (1997) found that injection of insulin into fasting mice rapidly returned the elevated liver glutaminase mRNA levels to normal levels.

5.1.4. Skeletal muscle

We take the same approach to modeling the modulation of Gln transport by cortisol as we did in the dexamethasone section; this is acceptable because glutamine transport alters rapidly in response to glucocorticoids (Hundal et al., 1991). Glutamine synthetase has a half-life near 24 h (Miller and Carrino, 1980) and hence responds more slowly. Therefore, we introduce a variable u for its upregulation which evolves according to Eq. (28); recall that g models cortisol concentration. The dependence of the velocity of the glutamine synthetase reaction on u is given in Table 6. We assume that Glu transport into skeletal muscle remained unaltered over the time course of the APAP simulations as the shift from the use of plasma Glu to the use of Glu generated from BCAA depends on muscle protein catabolism, a longer-term effect of glucocorticoids.

$$\frac{du}{dt} = \frac{\ln(2)}{24}(1.65g - u) \tag{28}$$

We model the exchange of Gln between mitochondria and the cytosol, not by introducing a separate compartment for

mitochondrial Gln, but by treating mitochondrial Gln as another variable associated with the muscle compartment. We call this variable *mitoGln*. The equations for cytosolic and mitochondrial Gln in skeletal muscle are given below.

$$\frac{d[smGln]}{dt} = \left(\frac{vB}{vSM}\right) V_{sm,glnin}([bGln]) - V_{sm,glnout}([smGln]) + V_{GS}([smGlu]) - k_{Gln,cm}[smGln] + k_{Gln,mc}[mitoGln] \quad (29)$$

$$\frac{d[mitoGln]}{dt} = k_{Gln,cm}[smGln] - k_{Gln,mc}[mitoGln] \quad (30)$$

5.1.5. Blood plasma

We assume that beginning 2.5 h after APAP overdose, cystine begins to be released into the blood plasma from the breakdown of fibrillin-1 protein found in liver vessel walls and portal tract connective tissue (Dubuisson et al., 2001); fibrillin is 14% cysteine and cysteine once entering plasma is rapidly oxidized to cystine. Fibrillin is broken down by elastase released by neutrophils. We assume that this cystine flux into the blood plasma, denoted by *cys2in*, approaches a maximal value of 3333 μM/h after a few hours, and then exponentially decays to zero beginning 7.5 h after APAP overdose. The equation for plasma cystine was given earlier, in the section on the cystine–glutamate antiporter. The equation for plasma cysteine is given below.

$$\frac{d[bCys]}{dt} = d_{deg}[bGSH] - V_{cysin}([bCys]) - k_{p,cysloss}[bCys] + 240\left(\frac{[bGSH]}{12.4}\right) k_{Cys2,Cys} \frac{[Cys_2]}{[Cys_2]+60} - 2k_{Cys,Cys2}[bCys] + cysin(t) \quad (31)$$

We assume that after 6 h, the rate of glutamine loss from the blood plasma compartment begins to increase, plateauing at a value 450% greater than under normal circumstances and then returning to normal with falling cortisol levels. This is to reflect increased uptake by the small intestine due to elevated cortisol, and increased uptake by immunologic cells associated with the inflammatory response. Six hours after APAP overdose is approximately the time at which liver neutrophil accumulation in mice undergoing APAP overdose was found to attain half its maximal value (Lawson et al., 2000). We assume the same alteration in the rate of Glu loss from blood plasma as for dexamethasone administration.

Table 6 summarizes the alterations in model parameters in response to APAP overdose.

5.2. Simulation of Hong experiments

Fig. 9 compares model solutions for liver GSH concentration and plasma Gln concentration during APAP overdose with data collected by Hong et al. (1992). Currently, ER rescue protocols assume that only cysteine is rate-limiting for GSH production and hence only *N*-acetylcysteine is given intravenously. Hong speculated that glutamine, which is converted to glutamate in the liver via glutaminase, might also be beneficial in maintaining GSH levels.

Hong gave rats either total parenteral nutrition for 5 days (control group) or parenteral nutrition supplemented with glutamine; on the fifth day a large overdose of acetaminophen was injected peritoneally (400 mg/kg). Animals were killed at 0, 1, 6, 9, and 24 h after overdose and liver glutathione and plasma glutamine concentrations were determined. Glutathione was far less depleted in the supplemented group, with the concentration returning to a normal value after 9 h; at 9 h the control group had only recovered 2/3 the normal concentration. After 24 h, both groups had higher then normal concentrations of glutathione, more so in the supplemented group. Mortality after 24 h was nearly one-half in the control group versus

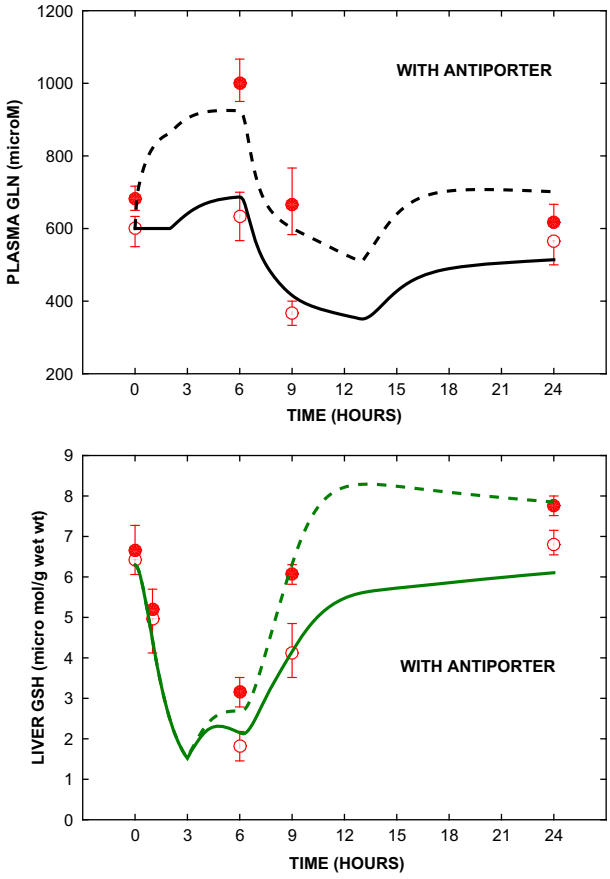

Fig. 9. Plasma Gln and liver GSH computed by the model in response to APAP overdose when the cystine–glutamate antiporter is expressed. Top panel shows the time course of plasma Gln computed by the model in response to an acetaminophen (APAP) overdose at $t=0$ when the initial condition for a control rat is used (*black*, *solid*) and when the initial condition for a Gln-supplemented rat is used (*black*, *dashed*). Bottom panel shows the computed time courses of liver GSH for the control rat (*green*, *solid*) and supplemented rat (*green*, *dashed*). Data collected by Hong et al. (1992) for control rats (*red*, *hollow*) and for Gln-supplemented rats (*red*, *solid*) are also plotted. The agreement between the model and Hong's data is excellent.

approximately 15% in the supplemented group (based on those animals which were selected to be killed at 24 h after overdose).

To compare Hong's results with model simulations, we assume that the additional Gln infused into the supplemented group over the 5-day period was stored mainly as free Gln in the skeletal muscle. Another possibility is that the additional glutamine received by the supplemented group was effectively stored as glutamate: studies with mouse skeletal muscle cells found that culturing the cells with elevated external glutamine downregulated the expression of glutamine synthetase (Huang and Wang, 2007). This could result in a surplus of Glu in skeletal muscle being on hand which is converted to Gln once an upregulation in glutamine synthetase is triggered during the response to APAP overdose. In this first paper we shall not explore this idea, but will make the simpler assumption that Gln itself is stored in muscle. Results for the control group were compared with the solution computed using the initial condition for the normal rat, and results for the supplemented group were compared with the solution computed using an initial condition in which muscle Gln was set to be 70% larger than normal.

In general, the agreement between model solutions and Hong's data is good (see Fig. 9). The empirically observed time course of plasma Gln concentration can be accounted for by the scenario

assumed by the model: a surge in cortisol beginning 2 h after APAP overdose which triggers a nearly immediate release of muscle Gln, followed by a dramatic increase in Gln uptake a few hours later by the small intestine and cells associated with the immune response. About 12 h later, after the peak of liver damage, the system normalizes and plasma Gln slowly approaches normal values.

The time course of liver GSH concentration found by Hong can be explained by a scenario in which the induction of the cystine–glutamate antiporter commences a few hours after overdose, increasing Cys and decreasing Glu in liver to the point where Glu becomes rate-limiting for the GCL reaction. Hence, the additional liver Glu present in the Gln-supplemented group results in a significantly greater amount of GSH. NAPQI begins to decline 6 h after overdose, at which point GSH rebounds dramatically and in fact exceeds its usual concentration even in controls; this effect is explicable in terms of the upregulation of the GCL reaction.

If we do not assume the induction of the cystine–glutamate antiporter, the model predicts that Gln supplementation has no power to preserve liver GSH levels against depletion; see Fig. 10. This is because under the model, in the absence of the antiporter it is always cysteine which is rate-limiting. The model predicts a depletion of liver GSH greater than occurred for Hong's control rats, suggesting that the cystine–glutamate antiporter is important for the preservation of liver GSH levels even under typical overdose conditions where no special supplementation is given. In the absence of the antiporter, GSH levels are predicted to be higher in the Gln-supplemented group 24 h after overdose, and both control and supplemented rats are predicted to have higher GSH levels than were seen in Hong's rats. This is because the large quantity of cystine entering the blood plasma remains there and eventually is reduced to cysteine which can enter the liver. Hence, there is an abundance of cysteine in liver and substantially upregulated glutamate–cysteine ligase. We note that hepatocytes passing through a period of such intense GSH depletion (and reduced ability to remove NAPQI) are unlikely to survive to the 24-h point; what the model predicts is the time course of GSH in those cells which do happen to survive.

Comparing the top panels of Figs. 9 and 10, we see that the presence or absence of the cystine–glutamate antiporter has no observable effect on the time course of Gln in plasma for either the control rats or the Gln-supplemented rats. Liver-type glutaminase (but not kidney-type) is not inhibited by its product, glutamate (Curthoys and Watford, 1995). Hence, although expression of the cystine–glutamate antiporter depletes liver Glu, this does not serve to increase the velocity at which Gln is consumed by the glutaminase reaction. As it has no impact on the concentration of Gln in liver, the cystine–glutamate antiporter has no impact on the concentration of Gln in plasma.

Our model suggests a scenario by which the sterile inflammatory response following APAP overdose works together with the expression of the cystine–glutamate antiporter to effect a partial preservation of liver GSH levels. Elastase released by neutrophils breaks down fibrillin protein in liver vessel walls and liberates a large quantity of cysteine into plasma, where it is rapidly oxidized to cystine. This cystine enters the liver via the antiporter where it is rapidly reduced to cysteine and incorporated into GSH. Without the action of the antiporter, liver GSH levels suffer greater depletion than was observed by Hong et al. (1992) in control rats. Including the antiporter results in excellent agreement with Hong's data. The model also explains why GSH levels were better preserved in Gln-supplemented rats relative to controls: the action of the antiporter depletes liver Glu, and Gln is a Glu precursor.

We note that our goal in this first paper is to lay out a possible scenario by which liver GSH levels may recover after overdose in those species in which APAP-induced liver damage occurs; we have used the Wistar rat as the model organism. Different species and strains differ in their values for some of the biochemical parameters appearing in our model; there are also gender differences. The model

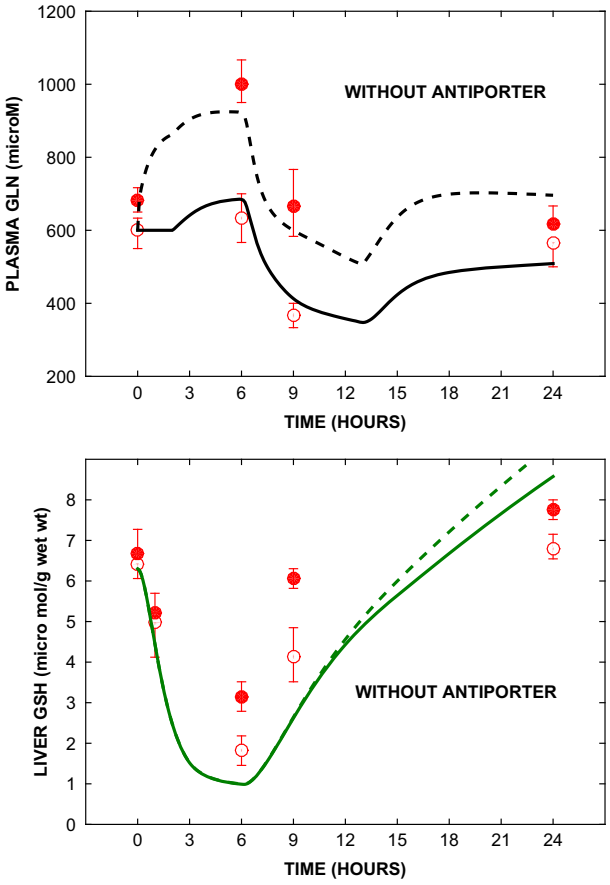

Fig. 10. Plasma Gln and liver GSH computed by the model in response to APAP overdose when the cystine/glutamate antiporter is not expressed, cf. Fig. 9; the model without the antiporter does not predict a preservation of liver GSH for Gln-supplemented rats relative to controls, consistent with Cys being the rate-limiting substrate for GSH formation. The model also predicts much lower GSH levels for both groups than found by Hong et al. for control rats except near the 24-h mark; this shows that the action of the antiporter is crucial for the recovery of liver GSH levels even under normal (non-supplemented) circumstances. Hepatocytes are unlikely to survive to the 24-h mark in such a scenario but for those that do, elevated GSH levels are predicted due to the abundance of cysteine in blood plasma generated from cystine which could not be taken up by liver during the acute stage of the overdose; see text.

can be used as a tool for exploring how these differences at the biochemical level translate into differences in aspects of response to APAP overdose which interest us, such as the liver glutathione concentration as a function of time. For example, in female mice there is a greater upregulation of γ-glutamyl cysteine ligase (GCL) in response to APAP overdose than in males and it is believed that this is responsible for the faster recovery of liver GSH levels seen in females (Masubuchi et al., 2011; McConnachie et al., 2007; Du et al., 2014). Fig. 11 compares the model solution for the control rat undergoing APAP overdose presented in Fig. 9 (black curve, labeled here as "male") with the solution obtained (blue curve, labeled here as "female") when V_{max} for the upregulated GCL reaction is given by

$$V_{max} = 3825\left(1+3\left(\frac{t-2}{t+2}\right)\right) \tag{32}$$

Compare with Table 6. The model confirms that a more dramatic induction of GCL in response to APAP overdose is sufficient to cause significantly faster recovery of GSH levels.

6. Discussion

We have developed a mathematical model of glutathione metabolism in rat liver which features the interactions among the

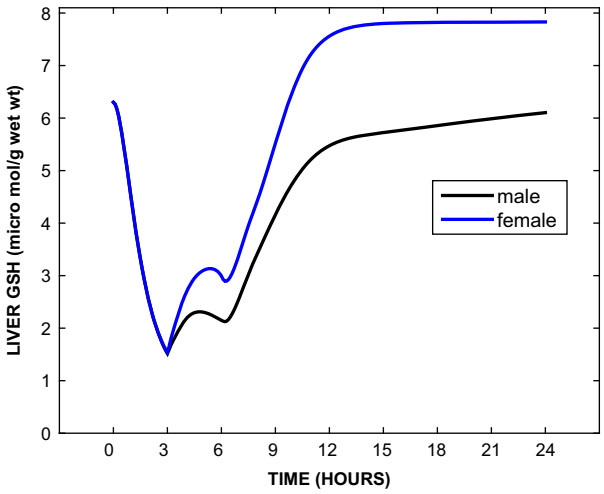

Fig. 11. Greater induction of GCL in response to APAP overdose results in faster recovery of liver GSH. The GCL reaction is upregulated during APAP overdose. Shown is a comparison of the time course of liver GSH in the control rat *(black)* of Fig. 9, for which a certain degree of GCL upregulation was assumed, with the time course obtained when the model is changed by assuming an even greater upregulation of GCL (*blue*); for precise values see text. The black and blue curves are labeled "male" and "female" respectively in reference to the situation in mice, in which female mice experience greater induction of GCL during APAP overdose than do male mice. Consistent with experimental findings, the model predicts faster recovery of GSH levels in females.

liver, blood plasma, and skeletal muscle. Where available, kinetic parameters for reaction velocities and amino acid transport rates were taken from the literature. Our inclusion of skeletal muscle stems from its role as a large supplier of Gln in plasma.

Cellular metabolism is an extremely complicated process and in seeking to devise a model simple enough to yield insight, we had to be selective in deciding which organs and which reactions within them to model explicitly. For example, perivenous scavenger cells of the liver contain glutamine synthetase and can take up vascular Glu and convert it to Gln. However, as these cells constitute only 7% of hepatocytes, we did not include them in the model. In spite of such simplifications, the model is able to explain many experimentally observed phenomena.

When parameters are chosen to reflect metabolism under normal physiologic conditions, our model reproduces the time course of decline in liver glutathione over 48 h observed during fasting, as well as its diurnal variation under fed conditions. When parameters are given functional dependencies on dexamethasone concentration (a synthetic glucocorticoid) consistent with information in the literature, the model correctly reproduces alterations in metabolism resulting from a 9-day course of dexamethasone injection. These alterations are consistent with a scenario of increased gluconeogenesis known to occur during catabolic states and believed to be mediated by glucocorticoids. The model also explains the linear decline in muscle Gln concentration to about half its normal value in terms of dexamethasone's alteration of muscle Gln transport parameters.

The model is consistent with data collected by Hong et al. (1992) on plasma Gln and liver GSH concentrations in rats undergoing APAP overdose, and explains the preservation of GSH in Gln-supplemented rats relative to controls via the action of the cystine/glutamate antiporter. This antiporter, which is not normally expressed in hepatocytes, increases the concentration of liver Cys while decreasing the concentration of liver Glu to the point that Cys is no longer rate-limiting for GSH synthesis, as it is under normal conditions. The current rescue protocol for patients presenting to the ED with APAP overdose is infusion with NAC, and our results suggest that this could be improved by inclusion of Gln, a possibility we will explore in a subsequent paper. We note that supplementation with Glu itself failed to have therapeutic value (Saito et al., 2010), consistent with the fact that most liver cells cannot take up vascular glutamate, this ability being confined to the perivenous cells (Kilberg and Haussinger, 1992).

In what follows we propose a possible mechanism for the physiological changes seen in low CG syndrome suggested to us by simulation experiments with our model; first, we review relevant facts. Under normal conditions plasma cystine concentration is significantly correlated with the rate of cystine release from skeletal muscle, which occurs in the post-absorptive state (Droege and Holm, 1997) due to the breakdown of muscle protein. This suggests that the muscle-wasting seen in low CG disorders results in an increased release of cystine into plasma. Furthermore, glucocorticoids are believed to mediate the increased skeletal muscle breakdown defining the catabolic state, and the primary glucocorticoid is cortisol; cortisol promotes protein breakdown in muscle, skin, and connective tissues (O'Toole, 2003) and these are among the tissues richest in cystine. This suggests that muscle-wasting is triggered by elevated cortisol levels which serve to transfer cystine in muscle and other tissues to plasma. Direct support for this was found by Kinscherf et al. (1996) in their study of healthy human subjects undergoing a program of anaerobic exercise for several weeks: subjects with low baseline plasma Gln and cystine concentrations (and only these subjects) showed a decrease in body cell mass over the observation period, at the end of which plasma cystine had increased, sometimes to higher-than-normal levels, and this increase in plasma cystine was strongly correlated with an increase in plasma Gln.

Cortisol is an anti-inflammatory hormone which serves to keep the inflammatory response in check; if levels are elevated in low CG-syndrome disorders, this suggests that the syndrome is accompanied by a state of inflammation either chronic or acute. Certainly this is the case for sepsis. In experimental models of inflammatory conditions, the cystine/glutamate antiporter has been found to be expressed in the neutrophils and macrophages infiltrating the site of inflammation (Nabeyama et al., 2010), suggesting a consumer for the increased release of cystine into plasma. Furthermore, in their course of action neutrophils release reactive oxygen species, which can result in a state of oxidative stress (Peake and Suzuki, 2004); oxidative stress has been found to induce the cystine/glutamate antiporter in a number of tissues (Conrad and Sato, 2012).

Taken together, these facts suggest to us that many low CG-syndrome disorders are accompanied by a state of inflammation which is the primary cause of the changes characterizing the syndrome: elevated cortisol increases the rate of release of Gln from skeletal muscle, but also increases its rate of uptake by small intestine; this, combined with the uptake of Gln by immunologic tissues ultimately causes plasma Gln to drop. Cortisol encourages the breakdown of skeletal muscle protein, increasing the release of cystine into plasma; however, the uptake of cystine by the cystine/glutamate antiporter ultimately causes plasma cystine to drop. The action of the antiporter pushes Glu out of cells and into plasma, causing plasma Glu to rise. In a rat model of breast cancer, Klimberg et al. (1996) found that supplementation with Gln effected a dramatic increase in natural killer (NK) cell activity and a dramatic reduction in tumor growth; in previous studies they found a dependence of NK cell activity on Gln levels in vivo and in vitro. This leads us to suggest that the decreased NK cell activity seen in low CG syndrome is the result of reduced plasma Gln.

Droege et al. propose an alternative explanation (Droege and Holm, 1997). Under their scenario, the normal release of cystine from skeletal muscle is actually reduced in low CG-syndrome disorders, causing a reduction in the plasma cystine level and ultimately cysteine concentration in liver. Since the catabolism of cysteine to sulfate in liver releases protons which scavenge the HCO_3^- anions needed to synthesize urea from NH_4^+, a lowered liver cysteine drives

up production of urea. The two fates of ammonium ions in liver are the formation of urea or the formation of Gln. Hence, a lowered plasma cystine concentration results in lowered liver Gln synthesis and release into plasma, ultimately lowering plasma Gln.

We agree that a lowered liver cysteine may be the driving force behind the increased urea production observed in low CG-syndrome disorders, and that the increased incorporation of ammonium ions into urea will reduce synthesis of Gln in liver. However, only the perivenous scavenger cells, which constitute 7% of hepatocytes, are capable of synthesizing Gln (Kilberg and Haussinger, 1992) so we believe that it is unlikely this is responsible for the lowered plasma Gln. Furthermore, a number of studies indicate that the liver is not a major contributor to the plasma Gln pool in healthy rats or humans (Hensley et al., 2013). For these reasons, we believe that it is more likely that the drop in plasma Gln observed in low CG conditions is due not to decreased release from liver but rather to increased uptake by the small intestine and immunologic tissues.

The ability of NAC supplementation to halt the reduction of body cell mass/body fat ratio seen in healthy subjects with low plasma Gln and cystine subjected to anaerobic exercise (Kinscherf et al., 1996) and its ability to effect a sturdy increase in plasma Gln in HIV-infected patients (Droege and Holm, 1997) suggests that some degree of inflammation is present in these conditions and that NAC can reduce it. Evidence indicates that HIV-infected patients are under chronic oxidative stress (Pace and Leaf, 1995) and have elevated cortisol levels (Christeff et al., 1997). Bloomer and Goldfarb (2004) have found that intense anaerobic exercise can generate oxidative stress; such exercise is associated with elevated plasma cortisol and pro-inflammatory cytokines. We hypothesize that oxidative stress may induce an inflammatory response and increase cortisol levels, and that NAC's role as a precursor of glutathione, the major antioxidant, explains its observed effects. Similarly, glutamine's ability to increase GSH synthesis when intracellular Glu is depleted via the action of the cystine/glutamate antiporter may explain why Gln supplementation has been found to counteract skeletal muscle Gln depletion and protein breakdown in catabolic states. In future work we plan to test these hypotheses by assuming a dependency of glucocorticoid level on redox status and investigating the model's response to oxidative stress.

Competing interests

The authors declare that they have no competing interests.

Acknowledgments

This research was supported by NSF Grants EF-1038593 (HFN, MCR) and DMS-0943760 (LMB, MCR), and NIH Grant R01 ES019876 (HFN, MCR).

References

Allan, E.H., Titheradge, M.A., 1984. Effect of treatment of rats with dexamethasone in vivo on gluconeogenesis and metabolite compartmentation in subsequently isolated hepatocytes. Biochem. J. 219, 117–123.
Ardawi, M.S.M., Jamal, Y.S., 1990. Glutamine metabolism in skeletal muscle of glucocorticoid-treated rats. Clin. Sci. 79, 139–147.
Ardawi, M.S.M., Majzoub, M.F., Newsholme, E.A., 1988. Effect of glucocorticoid treatment on glucose and glutamine metabolism by the small intestine of the rat. Clin. Sci. 75, 93–100.
Asola, M.R., Virtanen, K.A., Peltoniemi, P., Nagren, K., Yu, M., Mattila, K., Jyrkkio, S., Metsarinne, K., Nuutila, P., Knuuti, J., 2002. Amino acid uptake in the skeletal muscle measured using [11C]methylaminoisobutyrate (MEAIB) and PET. Eur. J. Nucl. Med. Mol. Imaging 29, 1485–1491.
Aw, T.Y., Ookhtens, M., Ren, C., Kaplowitz, N., 1986. Kinetics of glutathione efflux from isolated rat hepatocytes. Am. J. Physiol. Gast. Liver 250, G236–G243.
Baird, F.E., Beattie, K.J., Hyde, A.R., Ganapathy, V., Rennie, M.J., Taylor, P.M., 2004. Bidirectional substrate fluxes through the system N (SNAT5) glutamine transporter may determine net glutamine flux in rat liver. J. Physiol. 559, 367–381.
Bannai, S., 1984. Transport of cystine and cysteine in mammalian cells. Biochim. Biophys. Acta 779, 289–306.
Bannai, S., Takada, A., Kasuga, H., Tateishi, N., 1986. Induction of cystine transport activity in hepatocytes by sulfobromophthalein and other electrophilic agents. Hepatology 6, 1361–1368.
Bartoli, G.M., Sies, H., 1978. Reduced and oxidized glutathione efflux from liver. FEBS Lett. 86, 89–91.
Bloomer, R.J., Goldfarb, A.H., 2004. Anaerobic exercise and oxidative stress: a review. Can. J. Appl. Physiol. 29, 245–263.
Boelens, P.G., Nijveldt, R.J., Houdijk, A.P.J., Meijer, S., van Leeuwen, P.A.M., 2001. Glutamine alimentation in catabolic state. J. Nutr. 131, 2569S–2577S.
Carmagnol, F., Sinet, P.M., Jerome, H., 1983. Selenium-dependent and non-selenium-dependent glutathione peroxidases in human tissue extracts. Biochim. Biophys. Acta 759, 49–57.
Christeff, N., Gherbi, N., Mammes, O., Dalle, M.T., Gharakhanian, S., Lortholary, O., Melchior, J.C., Nunez, E.A., 1997. Serum cortisol and DHEA concentrations during HIV infection. Psychoneuroendocrinology 22, S11–S18.
Chung-Bok, M.I., Vincent, N., Jhala, U., Watford, M., 1997. Rat hepatic glutaminase: identification of the full coding sequence and characterization of a functional promoter. Biochem. J. 324, 193–200.
Conrad, M., Sato, H., 2012. The oxidative stress-inducible cystine/glutamate antiporter, system x_c^-: cystine supplier and beyond. Amino Acids 42, 231–246.
Curthoys, N.P., Watford, M., 1995. Regulation of glutaminase activity and glutamine metabolism. Annu. Rev. Nutr. 15, 133–159.
Cynober, L.A., Moore, F.A., 2003. Nutrition and Critical Care. Karger Medical and Scientific Publishers.
Droege, W., Holm, E., 1997. Role of cysteine and glutathione in HIV infection and other diseases associated with muscle wasting and immunological dysfunction. FASEB J. 11, 1077–1089.
Du, K., Williams, C.D., McGill, M.R., Jaeschke, H., 2014. Lower susceptibility of female mice to acetaminophen hepatotoxicity: role of mitochondrial glutathione, oxidant stress and c-jun N-terminal kinase. Toxicol. Appl. Pharmacol. 281, 58–66.
Dubuisson, L., Lepreux, S., Bioulac-Sage, P., Balabaud, C., Costa, A.M., Rosenbaum, J., Desmouliere, A., 2001. Expression and cellular localization of fibrillin-1 in normal and pathological human liver. J. Hepatol. 34, 514–522.
Elgadi, K.M., Souba, W.W., Bode, B.P., Abcouwer, S.F., 1997. Hepatic glutaminase gene expression in the tumor-bearing rat. J. Surg. Res. 69, 33–39.
Ellen, Friday, Robert, Oliver III, Francesco, Turturro, Tomas, Welbourne, 2012. Role of Glutamate Dehydrogenase in Cancer Growth and Homeostasis, Dehydrogenases, In: Rosa Angela Canuto (Ed.), InTech, http://dx.doi.org/10.5772/48606. ISBN: (978-953-307-019-3.) Available from: ⟨http://www.intechopen.com/books/dehydrogenases/role-of-glutamate-dehydrogenase-in-cancergrowth-and-homeostasis⟩.
Fork, C., Bauer, T., Golz, S., Geerts, A., Weiland, J., Turco, D.D., Schoemig, E., Gruendemann, D., 2011. OAT2 catalyses efflux of glutamate and uptake of orotic acid. Biochem. J. 436, 305–312.
Garrel, D., Patenaude, J., Nedelec, B., Samson, L., Dorais, J., Champoux, J., d'Elia, M., Bernier, J., 2003. Decreased mortality and infectious morbidity in adult burn patients given enteral glutamine supplements: a prospective, controlled, randomized clinical trial. Crit. Care Med. 31, 2444–2449.
Gebhardt, R., Kleemann, E., 1987. Hormonal regulation of amino acid transport system N in primary cultures of rat hepatocytes. Eur. J. Biochem. 166, 339–344.
Gebhardt, R., Mecke, D., 1983. Glutamate uptake by cultured rat hepatocytes is mediated by hormonally inducible, sodium-dependent transport systems. FEBS Lett. 161, 275–278.
Griffith, O.W., 1999. Biologic and pharmacologic regulation of mammalian glutathione synthesis. Free Radic. Biol. Med. 27, 922–935.
Haussinger, D., 1986. Regulation of hepatic ammonia metabolism: the intercellular glutamine cycle. Adv. Enzyme Regul. 25, 159–180.
Haussinger, D., Soboll, S., Meijer, A.J., Gerok, W., Tager, J.M., Sies, H., 1985. Role of plasma membrane transport in hepatic glutamine metabolism. Eur. J. Biochem. 152, 597–603.
Haussinger, D., Stoll, B., Stehle, T., Gerok, W., 1989. Hepatocyte heterogeneity in glutamate metabolism and bidirectional transport in perfused rat liver. Eur. J. Biochem. 185, 189–195.
Hell, R., Bergmann, L., 1990. γ-Glutamylcysteine synthetase in higher plants: catalytic properties and subcellular localization. Planta 180, 603–612.
Hensley, C.T., Wasti, A.T., DeBerardinis, R.J., 2013. Glutamine and cancer: cell biology, physiology, and clinical opportunities. J. Clin. Invest. 123, 3678–3684.
Hillesheim, W., Jaeschke, H., Neumann, H.G., 1995. Cytotoxicity of aromatic amines in rat liver and oxidative stress. Chem. Biol. Interact. 98, 85–95.
Hinson, J.A., Han-Hsu, H., Mays, J.B., Holt, S.J., McLean, P., Ketterer, B., 1984. Acetaminophen-induced alterations in blood glucose and blood insulin levels in mice. Res. Commun. Chem. Pathol. Pharmacol. 43, 381–391.
Hong, R.W., Rounds, J.D., Helton, W.S., Robinson, M.K., Wilmore, D.W., 1992. Glutamine preserves liver glutathione after lethal hepatic injury. Ann. Surg. 215, 114–119.
Huang, Y.F., Wang, Y., Watford, M., 2007. Glutamine directly downregulates glutamine synthetase protein levels in mouse C2C12 skeletal muscle myotubes. J. Nutr. 137, 1357–1362.
Hundal, H.S., Babij, P., Taylor, P.M., Watt, P.W., Rennie, M.J., 1991. Effects of corticosteroid on the transport and metabolism of glutamine in rat skeletal muscle. Biochim. Biophys. Acta 1092, 376–383.

Hutson, S.M., Sweatt, A.J., LaNoue, K.F., 2005. Branched-chain amino acid metabolism: implications for establishing safe intakes. J. Nutr. 135, 1557S–1564S.
Inoue, M., Kinne, R., Tran, T., Arias, I., 1984. Glutathione transport across hepatocyte plasma membranes. Eur. J. Biochem. 138, 491–495.
Jaeschke, H., Wendel, A., 1985. Diurnal fluctuation and pharmacological alteration of mouse organ glutathione content. Biochem. Pharmacol. 34, 1029–1033.
Jaeschke, H., Williams, C.D., Ramachandran, A., Bajt, M.L., 2012. Acetaminophen hepatotoxicity and repair: the role of sterile inflammation and innate immunity. Liver Int. 32, 8–20.
Jucker, B.M., Lee, J.Y., Shulman, R.G., 1998. In vivo ^{13}C NMR measurements of hepatocellular tricarboxylic acid cycle flux. J. Biol. Chem. 273, 12187–12194.
Keener, J.P., Sneyd, J., 2009. Mathematical Physiology I: Cellular Physiology, second ed. Springer Science+Business Media, LLC, New York, USA.
Kilberg, M.S., Haussinger, D. (Eds.), 1992. Mammalian Amino Acid Transport, Plenum (an imprint of Springer), New York, USA.
Kinscherf, R., Hack, V., Fischbach, T., Friedmann, B., Weiss, C., Edler, L., Baertsch, P., Droege, W., 1996. Low plasma glutamine in combination with high glutamate levels indicate risk for loss of body cell mass in healthy individuals: the effect of N-acetyl-cysteine. J. Mol. Med. (Berl.) 74, 393–400.
Klimberg, V.S., Kornbluth, J., Cao, Y., Dang, A., Blossom, S., Schaeffer, R.F., 1996. Glutamine suppresses PGE2 synthesis and breast cancer growth. J. Surg. Res. 63, 293–297.
Klin, Y., Zlotkin, A., Boyko, M., Ohayon, S., Shapira, Y., Teichberg, V.I., 2010. Distribution of radiolabeled L-glutamate and D-aspartate from blood into peripheral tissues in naive rats: significance for brain neuroprotection. Biochem. Biophys. Res. Commun. 399, 694–698.
Kondo, T., Dale, G.L., Beutler, E., 1980. Glutathione transport by inside-out vesicles from human erythrocytes. Proc. Natl. Acad. Sci. 77, 6359–6392.
Kretzschmar, M., 1996. Regulation of hepatic glutathione metabolism and its role in hepatotoxicity. Exp. Toxicol. Pathol. 48, 439–446.
Latta, K., Augusteyn, R.C., 1984. The purification and properties of human lens glutathione reductase. Exp. Eye Res. 39, 343–354.
Lauterburg, B.H., Adams, J.D., Mitchell, J.R., 1984. Hepatic glutathione homeostasis in the rat: efflux accounts for glutathione turnover. Hepatology 4, 586–590.
Lawson, J.A., Farhood, A., Hopper, R.D., Bajt, M.L., Jaeschke, H., 2000. The hepatic inflammatory response after acetaminophen overdose: role of neutrophils. Toxicol. Sci. 54, 509–516.
Leweling, H., Breitkreuz, R., Behne, F., Staedt, U., Striebel, J., 1996. Hyperammonemia-induced depletion of glutamate and branched-chain amino acids in muscle and plasma. J. Hepatol. 25, 756–762.
Low, S.Y., Taylor, P.M., Hundal, H.S., Pogson, C.I., Rennie, M.J., 1992. Transport of L-glutamine and L-glutamate across sinusoidal membranes of rat liver: effects of starvation, diabetes and corticosteroid treatment. Biochem. J. 284, 333–340.
Lu, S.C., 1999. Regulation of hepatic glutathione synthesis: current concepts and controversies. FASEB J. 13, 1169–1183.
Lu, S.C., Ge, J.L., Kuhlenkamp, J., Kaplowitz, N., 1992. Insulin and glucocorticoid dependence of hepatic gamma-glutamylcysteine synthetase and glutathione synthesis in the rat. Studies in cultured hepatocytes and in vivo. J. Clin. Invest. 90, 524–532.
Masubuchi, Y., Nakayama, J., Watanabe, Y., 2011. Sex difference in susceptibility to acetaminophen hepatotoxicity is reversed by buthionine sulfoximine. Toxicology 287, 54–60.
McConnachie, L.A., Mohar, I., Hudson, F.N., Ware, C.B., Ladiges, W.C., Fernandez, C., Chatterton-Kirchmeier, S., White, C.C., Pierce, R.H., Kavanagh, T.J., 2007. Glutamate cysteine ligase modifier subunit deficiency and gender as determinants of acetaminophen-induced hepatotoxicity in mice. Toxicol. Sci. 99, 628–636.
Mendoza-Cozatl, D.G., Moreno-Sanchez, R., 2006. Control of glutathione and phytochelatin synthesis under cadmium stress. Pathway modeling for plants. J. Theor. Biol. 238, 919–936.
Miller, R.E., Carrino, D.A., 1980. Dibutyryl cyclic AMP decreases glutamine synthetase in cultured 3T3-L1 adipocytes. J. Biol. Chem. 255, 5490–5500.
Minet-Quinard, R., Moinard, C., Walrand, S., Villie, F., Normand, B., Vasson, M., Chopineau, J., Cynober, L., 2000. Induction of a catabolic state in rats by dexamethasone: dose or time dependency?#. J. Parent. Enter. Nutr. 24, 30–36.
Moslen, M.T., Smith, C.V., 1992. Free Radical Mechanisms of Tissue Injury. CRC Press, Inc..
Muratsubaki, H., Yamaki, A., 2011. Profile of plasma amino acid levels in rats exposed to acute hypoxic hypoxia. Indian J. Clin. Biochem. 26, 416–419.
Nabeyama, A., Kurita, A., Asano, K., Miyake, Y., Yasuda, T., Miura, I., Nishitai, G., Arakawa, S., Shimizu, S., Wakana, S., Yoshida, H., Tanaka, M., 2010. xCT deficiency accelerates chemically induced tumorigenesis. Proc. Natl. Acad. Sci. 107, 6436–6441.
Newsholme, Philip, 2001. Why is L-glutamine metabolism important to cells of the immune system in health, postinjury, surgery or infection? J. Nutr. 131, 2515S–2522S.
Ookhtens, M., Hobdy, K., Corvasce, M.C., Aw, T.Y., Kaplowitz, N., 1985. Sinusoidal efflux of glutathione in the perfused rat liver: evidence for a carrier-mediated process. J. Clin. Invest. 75, 258–265.
Ookhtens, M., Kaplowitz, N., 1998. Role of the liver in interorgan homeostasis of glutathione and cyst(e)ine. Semin. Liver Dis. 18, 313–329.
Ookhtens, M., Maddatu, T., 1991. Mechanism of changes in hepatic sinusoidal and biliary glutathione efflux with age in rats. Am. J. Physiol. 261, G648–G656.
Ookhtens, M., Mittur, A.V., Erhart, N.A., 1994. Changes in plasma glutathione concentrations, turnover, and disposal in developing rats. Am. J. Physiol. 266, R979–R988.
O'Toole, M.T. (Ed.), 2003. Miller–Keane Encyclopedia and Dictionary of Medicine, Nursing, and Allied Health, seventh ed. Saunders.
Pace, G.W., Leaf, C.D., 1995. The role of oxidative stress in HIV disease. Free Radic. Biol. Med. 19, 523–528.
Peake, J., Suzuki, K., 2004. Neutrophil activation, antioxidant supplements and exercise-induced oxidative stress. Exerc. Immunol. Rev. 10, 129–141.
Reed, M.C., Thomas, R.L., Pavisic, J., James, S.J., Ulrich, C.M., Nijhout, H.F., 2008. A mathematical model of glutathione metabolism. Theoret. Biol. Med. Model. 5, 8.
Richman, P.G., Meister, A., 1975. Regulation of gamma-glutamyl–cysteine synthetase by non-allosteric feedback inhibition by glutathione. J. Biol. Chem. 250, 1422–1426.
Saito, C., Zwingmann, C., Jaeschke, H., 2010. Novel mechanisms of protection against acetaminophen hepatotoxicity in mice by glutathione and *N*-acetylcysteine. Hepatology 51, 246–254.
Savvides, S., Scheiwein, M., Bohme, C., Arteel, G., Karplus, P.A., Becker, K., Schirmer, R.H., 2002. Crystal structure of the antioxidant enzyme glutathione reductase inactivated by peroxynitrite. J. Biol. Chem. 277, 2779–2784.
Scheer, J.B., Mackey, A.D., Gregory III, J.F., 2005. Activities of hepatic and cytosolic mitochondrial forms of serine hydroxymethyltransferase and hepatic glycine concentration are affected by vitamin B-6 intake in rats. J. Nutr. 135, 233–238.
Seelig, G., Meister, A., 1985. Glutathione biosynthesis: gamma-glutamylcysteine synthetase from rat kidney. Methods Enzymol. 113, 379–399.
Siess, E.A., Brocks, D.G., Lattke, H.K., Wieland, O.H., 1977. Effect of glucagon on metabolite compartmentation in isolated rat liver cells during gluconeogenesis from lactate. Biochem. J. 166, 225–235.
Smith, R.J., Larson, S., Stred, S.E., Durschlag, R.P., 1984. Regulation of glutamine synthetase and glutaminase activities in cultured skeletal muscle cells. J. Cell. Physiol. 120, 197–203.
Stipanuk, M.H., Dominy Jr., J.E., Lee, J., Coloso, R.M., 2006. Mammalian cysteine metabolism: new insights into regulation of cysteine metabolism. J. Nutr. 136, 1652S–1659S.
Tateishi, N., Higashi, T., Shinya, S., Naruse, A., Sakamoto, Y., 1974. Studies on the regulation of glutathione level in rat liver. J. Biochem. 75, 93–103.
Wang, W., Wu, Z., Dai, Z., Yang, Y., Wang, J., Wu, G., 2013. Glycine metabolism in animals and humans: implications for nutrition and health. Amino Acids 45, 463–477.
Watford, M., 2008. Glutamine metabolism and function in relation to proline synthesis and the safety of glutamine and proline supplementation. J. Nutr. 138, 2003S–2007S.
Wu, G., Fang, Y., Yang, S., Lupton, J.R., Turner, N.D., 2004. Glutathione metabolism and its implications for health. J. Nutr. 134, 3.